ANNUAL REVIEWS

Annual Review of Biochemistry

Evolutionary Dynamics and Molecular Mechanisms of HORMA Domain Protein Signaling

Yajie Gu,[1] Arshad Desai,[1,2,3] and Kevin D. Corbett[1,4]

[1]Department of Cellular & Molecular Medicine, University of California San Diego, La Jolla, California, USA; email: kcorbett@ucsd.edu

[2]Section of Cell & Developmental Biology, Division of Biological Sciences, University of California San Diego, La Jolla, California, USA

[3]Ludwig Institute for Cancer Research, San Diego Branch, La Jolla, California, USA

[4]Department of Chemistry and Biochemistry, University of California San Diego, La Jolla, California, USA

Annu. Rev. Biochem. 2022. 91:541–69

First published as a Review in Advance on January 18, 2022

The *Annual Review of Biochemistry* is online at biochem.annualreviews.org

https://doi.org/10.1146/annurev-biochem-090920-103246

Keywords

mitosis, meiosis, spindle assembly checkpoint, meiotic recombination, translesion synthesis, shieldin, autophagy, cancer

Abstract

Controlled assembly and disassembly of multi-protein complexes is central to cellular signaling. Proteins of the widespread and functionally diverse HORMA family nucleate assembly of signaling complexes by binding short peptide motifs through a distinctive safety-belt mechanism. HORMA proteins are now understood as key signaling proteins across kingdoms, serving as infection sensors in a bacterial immune system and playing central roles in eukaryotic cell cycle, genome stability, sexual reproduction, and cellular homeostasis pathways. Here, we describe how HORMA proteins' unique ability to adopt multiple conformational states underlies their functions in these diverse contexts. We also outline how a dedicated AAA+ ATPase regulator, Pch2/TRIP13, manipulates HORMA proteins' conformational states to activate or inactivate signaling in different cellular contexts. The emergence of Pch2/TRIP13 as a lynchpin for HORMA protein action in multiple genome-maintenance pathways accounts for its frequent misregulation in human cancers and highlights TRIP13 as a novel therapeutic target.

Contents

1. INTRODUCTION

The HORMA domain was first identified in 1998 by Aravind and Koonin (1), who showed that three diverged proteins in *Saccharomyces cerevisiae* share a common fold: the meiotic recombination regulator Hop1, the DNA repair factor Rev7, and the spindle assembly checkpoint (SAC) protein Mad2 (the name HORMA comes from the initial letters of Hop1, Rev7, and Mad2). Between 2000 and 2008, foundational studies on Mad2 revealed the HORMA domain's unique capacity to adopt two distinct folded states (**Figure 1*a***) and showed how controlled assembly of Mad2-containing complexes underlies SAC signaling (2–4). This paradigm has informed the functional analysis of other HORMA proteins, including recently discovered bacterial family members. The developing picture of HORMA domain function is that these proteins default to an inactive open conformation that is poised for conversion to an active, partner-bound closed conformation; the resulting stable HORMA–partner complex initiates signaling, which is inactivated only upon disassembly of the complex by a dedicated ATPase remodeler protein.

HORMA: a conserved signaling domain named for three proteins (Hop1, Rev7, and Mad2) originally observed to share this domain

Spindle assembly checkpoint (SAC): a checkpoint pathway that produces the mitotic checkpoint complex at unattached kinetochores to delay mitotic exit

AAA+ ATPase: a broad family of hexameric motor proteins (ATPases associated with diverse cellular activities)

In this review, we begin by outlining the current understanding of HORMA protein evolution, with an ancestral bacterial immunity factor giving rise to a diverse set of eukaryotic signaling proteins. We next describe recent progress on diverse HORMA proteins that reveals striking mechanistic parallels among family members acting in distinct biological contexts. We pay particular attention to the AAA+ ATPase remodeler Pch2/TRIP13, which is now appreciated as a universal regulator of HORMA domains' conformational equilibrium and partner-protein binding. Finally, we discuss how the diverse functions of Pch2/TRIP13 in HORMA protein regulation complicate, but also clarify, our understanding of its contributions to human cancer.

2. EVOLUTIONARY HISTORY OF THE HORMA DOMAIN

While the HORMA domain was first defined by sequence similarities between Hop1, Rev7, and Mad2 (1), the full complement of eukaryotic HORMA proteins also includes a second SAC protein, p31^{comet} (5), and two autophagy proteins, Atg13 and Atg101 (6–9) (**Figure 1*b***, **Supplemental Table 1**). In 2015, a comparative genomics study in bacteria—led by HORMA domain codiscoverer L. Aravind (10)—reported putative HORMA domain proteins outside eukaryotes, encoded

Supplemental Material >

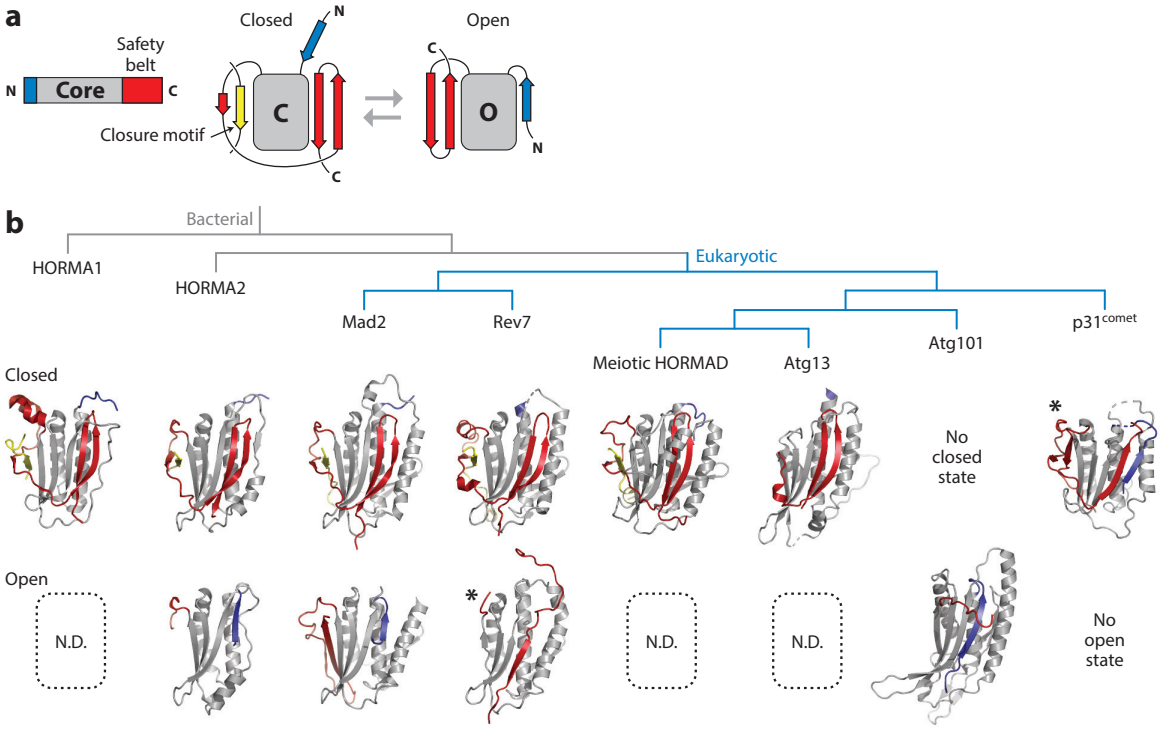

Biological pathway							
Bacterial anti-viral immunity		Spindle checkpoint	DNA repair	Meiotic recombination	Autophagy	Autophagy	Spindle checkpoint
Closure motif-containing binding partner(s)							
Infection signals?	Infection signals?	Mad1 Cdc20 Shugoshin	Rev3 SHLD3 CDH1?	Self (C-term) Axis core proteins	Atg9? Atg14?	Locked open	Self-closed
Dimer partner(s)							
–	–	Mad2 p31comet	Rev7 p31comet ?	?	Atg101	Atg13	Mad2
Pch2/TRIP13 substrate?							
+	+	+	+	+	?	–	Adapter

Figure 1

Structure, function, and evolution of HORMA domain proteins. (*a*, *left*) Schematic of the HORMA domain with the flexible N-terminal region colored blue and the C-terminal safety belt colored red. (*Right*) Schematic views of the two folded states of the HORMA domain. In the closed (C) conformation, the safety belt is wrapped around a bound closure motif peptide (*yellow*). In the open (O) conformation, the safety belt binds and blocks access to the closure motif binding site. (*b*, *top*) Evolutionary tree of HORMA domain proteins (adapted from Reference 26). Bacterial HORMA proteins fall into two families, HORMA1 and HORMA2 (the diverged HORMA3 family is not shown). Eukaryotic HORMA proteins form a monophyletic group within the HORMA2 family. (*Middle*) Structures of HORMA domain proteins in the closed conformation (with bound closure motifs) or the open conformation, colored as in panel *a*. Noncanonical structural states (open Rev7 and closed p31^{comet}) are indicated with asterisks. The Protein Data Bank identifiers for these structures are as follows: HORMA1, 6U7B (11); closed HORMA2–peptide 1, 6P8S (11); open HORMA2, 6P8O (11); closed Mad2–MBP1 peptide, 2V64 (27); open Mad2, 2V64 (27); closed Rev7–Rev3, 3ABE (142); open Rev7, 6KTO (29); closed meiotic HORMAD (HIM-3–HTP-3 motif #4), 4TZJ (97); Atg13, 5XV4 (28); Atg101, 5XV4 (28) –p31^{comet}, 2QYF (5). (*Bottom*) Known closure motif–containing binding partners for each HORMA protein family, dimerization binding partners (see **Figure 2*b***), and current knowledge of each proteins' regulation by Pch2/TRIP13. See **Supplemental Table 1** for a catalog of HORMA domain proteins in eukaryotic model organisms.

Supplemental Material >

in bacterial operons of unknown function. These proteins were recently shown to be bona fide HORMA proteins that play a key signaling role in a bacterial antiviral immunity pathway (11). Moreover, these bacterial operons encode an ortholog of the AAA+ ATPase remodeler Pch2/TRIP13, which in eukaryotes regulates signaling by multiple families of HORMA proteins (12–25). Phylogenetic analysis shows that eukaryotic HORMA and Pch2/TRIP13 proteins likely descended from their bacterial relatives (26), cementing the idea that HORMA proteins and Pch2/TRIP13 constitute an evolutionarily conserved functional module (**Figure 1*b***). Expansion of the HORMA family in eukaryotes subsequently enabled these proteins' integration into key chromosome maintenance, cell cycle, and homeostatic signaling pathways.

Closure motif: a short protein sequence that binds a closed HORMA protein; also called MIM (Mad2-binding motif) or RBM (Rev7-binding motif)

Mitotic checkpoint complex (MCC): a multiprotein complex generated at unattached kinetochores that binds and inhibits the anaphase promoting complex/cyclosome

Shieldin: a multi-protein complex that binds broken DNA ends and inhibits end resection, thereby inhibiting homologous recombination and promoting nonhomologous end joining

Kinetochore: a megadalton-scale protein complex that mediates attachment of mitotic chromosomes to microtubules and signals attachment status through the spindle assembly checkpoint

3. CONSERVED MECHANISMS OF HORMA DOMAIN SIGNALING

3.1. Conformational Conversion and Closure Motif Binding

The HORMA domain is a compact domain of ~200 amino acids whose core consists of a stable three-stranded β-sheet backed by three α-helices. The two edges of the core β-sheet serve as interaction sites for binding partners and for the domain's flexible N- and C-terminal regions. In the partner-bound closed conformation, a 6–10-amino-acid region of a binding partner, termed a closure motif, forms a short β-strand and binds along the C-terminal edge of the HORMA domain's core β-sheet. This interaction is stabilized when the flexible C terminus of the HORMA domain, termed the safety belt, wraps around the bound closure motif and associates with the opposite (N-terminal) edge of the core β-sheet (**Figure 2*a***). A HORMA domain–closure motif complex is therefore topologically linked, such that disassembly requires at least partial unfolding of the HORMA domain.

In nearly all HORMA-mediated signaling pathways, the closed HORMA domain–closure motif complex serves as the nucleus for assembly of larger signaling complexes like the mitotic checkpoint complex (MCC) (nucleated by Mad2–Cdc20) or the shieldin complex (nucleated by Rev7–SHLD3). A critical mechanistic puzzle, however, has been how these complexes initially assemble. Because of their topologically linked structure, HORMA domain–closure motif complexes cannot simply form through binding of a closure motif to a closed HORMA domain. Rather, assembly requires that the HORMA domain adopt what we term an unbuckled state, in which the C-terminal safety belt is disengaged from the HORMA domain core to allow access to the closure motif binding site (**Figure 2*a***). This unique requirement enables cells to tightly regulate assembly of HORMA domain–closure motif complexes in order to achieve highly specific signaling. In addition to the canonical closed conformation and the transient, partially unfolded unbuckled state, some HORMA proteins can also adopt a third, semistable conformation termed open. In this state, the C-terminal safety belt is docked against the closure motif binding site, and the HORMA domain N terminus—which is disordered in the closed conformation—docks against and stabilizes the N-terminal edge of the core β-sheet. In the best-understood HORMA protein, Mad2, the open state is critical for spindle checkpoint signaling: Open Mad2 (O-Mad2) is recruited to kinetochores and then stimulated to undergo conformational conversion, first to an unbuckled transition state and finally to the stable closed conformation bound to a closure motif in its binding partner Cdc20. Thus, HORMA domain signaling revolves around a complex energetic equilibrium between open, unbuckled, and closed conformations that is manipulated by cells to achieve signal activation and inactivation in different contexts (**Figure 2*a***).

3.2. HORMA Domain Dimerization

Another shared feature of HORMA domains is their ability to form homo- and heterodimers through a canonical interface composed of the N-terminal edge of the domain's β-sheet and a

neighboring α-helix (helix αC) (**Figure 2*b***). This interface has not been observed in bacterial HORMA proteins but exists in nearly all eukaryotic HORMA proteins, including Mad2 (27), p31^{comet} (5), the autophagy proteins Atg13 and Atg101 (7, 9, 28), and with some modifications, Rev7 (29). In all cases, the structure of the HORMA domain dimerization surface changes between these proteins' open and closed conformations, and dimer formation is therefore conformation specific. This property enables HORMA domain dimerization to serve as a conformational

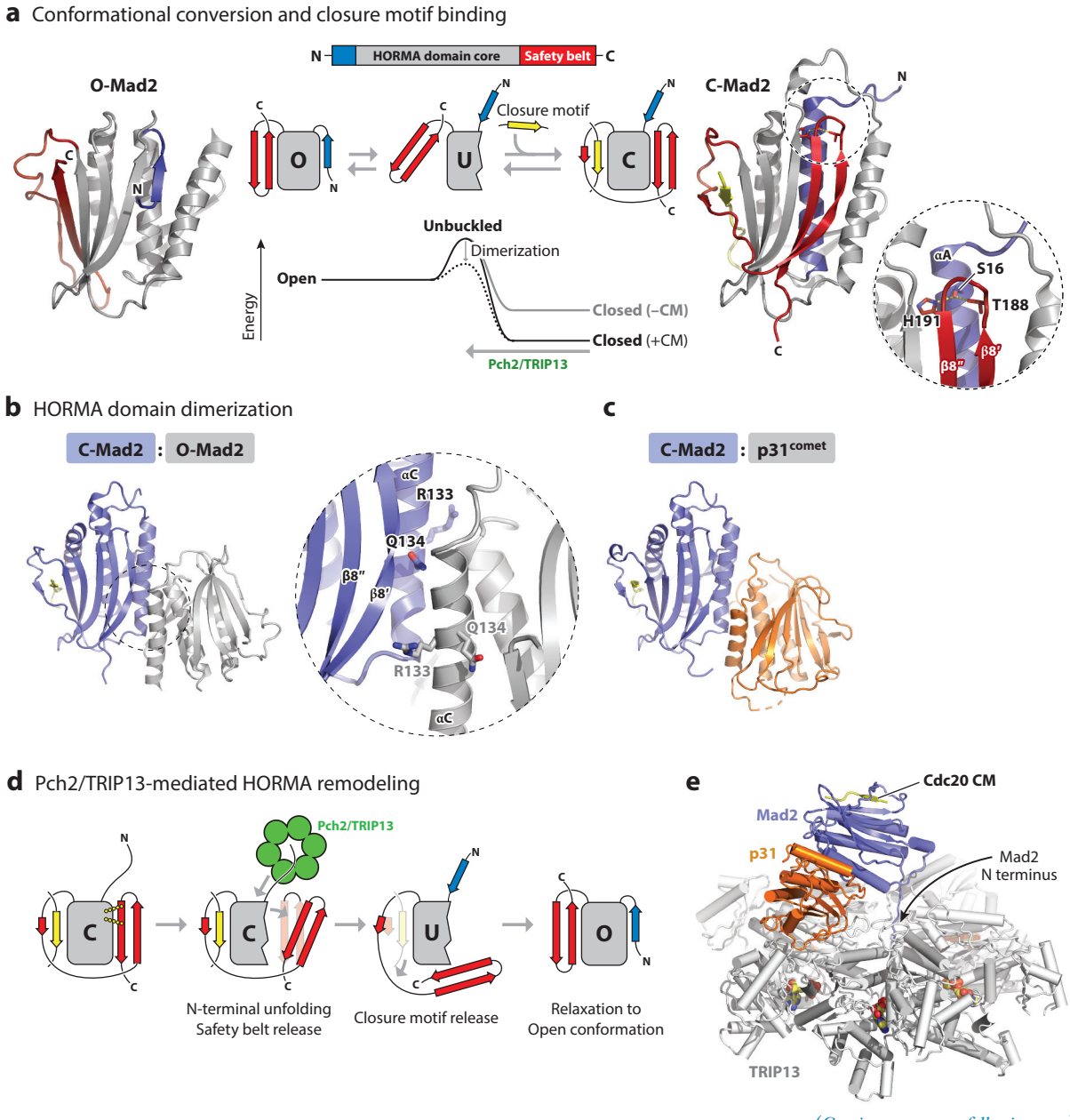

(Caption appears on following page)

Figure 2 (*Figure appears on preceding page*)

Mechanisms of HORMA domain signaling. (*a*) Conformational states and conformational conversion of Mad2. Three conformations are differentiated by the positions of the flexible N terminus (*blue*) and the C-terminal safety belt (*red*) with respect to the core β-sheet (*gray*). A closure motif (*yellow*) can bind concomitantly with a transition from the unbuckled (U) to the closed (C) conformation. Open and closed conformers of Mad2 [PDB ID: 2V64 (27)] are shown on either side. A close-up of C-Mad2 shows the conserved hydrogen bonding network linking the safety belt β-strands β8′ and β8″ to helix αA. (*Bottom center*) Relative thermodynamic stability of the open, unbuckled, and closed conformations. The closed conformation, lacking a bound closure motif (−CM), is less stable than the closure motif-bound form (+CM). (*b*) Overall and close-up views of the C-Mad2–O-Mad2 dimer [PDB ID: 2V64 (27)] with C-Mad2 colored blue, the MBP1 closure motif peptide yellow, and O-Mad2 gray. Shown as sticks are two Mad2 residues, R133 and Q134, whose mutation disrupts Mad2 dimer formation. Dimerization introduces strain in the O-Mad2 protomer, lowering the activation energy for conformational conversion to the closed state. (*c*) Structure of the C-Mad2–p31^{comet} dimer [PDB ID: 2QYF (5)] with C-Mad2 colored blue, the MBP1 closure motif peptide yellow, and p31^{comet} orange. (*d*) Schematic of Pch2/TRIP13-mediated HORMA domain conformational conversion [adapted from (23)]. Pch2/TRIP13 binds the disordered N terminus of a closed HORMA domain and unfolds a portion of helix αA, disrupting its interactions with the safety belt β-strands. Destabilization and disengagement of the safety belt from the HORMA domain core leads to closure motif release. Conformational conversion is completed when the HORMA domain relaxes into the open conformation. (*e*) Cryo-electron microscopy structure of the *Homo sapiens* TRIP13 hexamer (*white*) with bound ATP-γS (*yellow*) bound to its substrate complex, p31^{comet}–Mad2–Cdc20 closure motif (*orange*, *blue*, and *yellow*, respectively) [PDB ID: 6F0X (33)]. The flexible N terminus of C-Mad2 drapes into the TRIP13 hexamer pore. See **Supplemental Figure 1** for more details on Pch2/TRIP13 substrate interactions. Abbreviations: C, closed; CM, closure motif; O, open; PDB ID, Protein Data Bank identifier; U, unbuckled.

Supplemental Material >

readout, providing a way for other binding partners to sense and respond to conformational changes mediated by closure motif binding.

While the overall architecture of HORMA domain dimers is conserved across families, the roles of these dimers vary. Both Rev7 homodimers and Atg13–Atg101 heterodimers appear to serve as platforms for assembly of larger signaling complexes (see Section 4.5). In Mad2, however, dimerization plays two key roles to drive HORMA domain conformational changes and the assembly and disassembly of Mad2-containing signaling complexes. Specifically, dimerization of O-Mad2 with a closed Mad2 (C-Mad2)–Mad1 complex at unattached kinetochores introduces strain within the O-Mad2 protomer, lowering the activation energy for an open-to-closed conformational change that is coupled to closure motif binding (**Figures 2*a*** and **4**) (30). p31^{comet} uses an equivalent interaction to recognize C-Mad2 and recruit it to the Pch2/TRIP13 ATPase for closed-to-open conformational conversion (**Figure 2*b***) (5). Thus, HORMA domain dimerization is critical for both assembly and disassembly of Mad2-containing signaling complexes, in addition to serving as a general mode of conformation-specific HORMA domain assembly.

3.3. HORMA Domain Remodeling by Pch2/TRIP13

Assembly of HORMA domain–closure motif complexes is kinetically slow but ultimately energetically favorable (**Figure 2*a***). Disassembly of these complexes, however, generally requires energy input to partially unfold the HORMA domain and release the bound closure motif. Disassembly is mediated by Pch2/TRIP13, a member of the AAA+ ATPase remodeler superfamily (**Figure 2*d*,*e***). AAA+ ATPase remodelers function as ATP-powered pumps, with ATP hydrolysis driving coordinated conformational changes in the ring-shaped homohexameric complex that pull substrate proteins through a central pore to unfold them (31, 32). Whereas most AAA+ ATPase remodelers processively unfold their substrates from one terminus to the other, Pch2/TRIP13 recognizes the disordered N terminus of its closed HORMA domain substrate and unfolds only a portion of its N-terminal α-helix before disengaging (19, 23, 33). The molecular basis for disengagement after only partial HORMA unfolding is not known but may involve the inherent instability of the Pch2/TRIP13 hexamer and/or higher stability of the HORMA domain core relative to its N-terminal region. Curiously, bacterial Trip13 appears exquisitely adapted to partial HORMA

unfolding: Bacterial HORMA1 proteins have a conserved pattern of serine/threonine residues in their N-termini, and these residues are specifically engaged by conserved histidine residues in the pore loops of their cognate Trip13 enzymes (11). In all cases, partial unfolding of the HORMA protein's N-terminal α-helix in turn destabilizes the C-terminal safety belt, driving the protein into an unbuckled conformation while leaving the HORMA domain core intact (**Figure 2*d***) (34). In Mad2, and potentially other HORMA domain proteins, the resulting unbuckled intermediate then relaxes into the open conformation, resetting the pathway.

While the overall mechanism of HORMA–closure motif complex disassembly by Pch2/TRIP13 is conserved from bacteria to eukaryotes, the mode of substrate recognition varies (**Supplemental Figure 1**). In bacteria, HORMA protein recognition is mediated by a biosynthetic enzyme that binds Trip13 and positions the HORMA protein for unfolding (11). In eukaryotes, the HORMA protein p31^{comet} serves as a Pch2/TRIP13 adapter for several HORMA proteins, dimerizing with Mad2, Rev7, or a meiotic HORMAD protein in the closed conformation and recruiting it to Pch2/TRIP13 (**Figure 2*e***; for details, see Sections 4.2–4.4) (19, 23, 33, 35). In all cases, the adapter proteins bind the top surface of the Pch2/TRIP13 ATPase domain directly, rather than binding a family-specific N-terminal domain as with most other AAA+ ATPases (**Supplemental Figure 1**).

Meiotic HORMAD: general term for Hop1 and related HORMA domain proteins that function in meiotic recombination

CBASS: a newly described bacterial antiviral immunity pathway (cyclic oligonucleotide-based antiphage signaling system)

Supplemental Material >

4. BIOLOGICAL ROLES OF HORMA PROTEINS

To date, HORMA proteins have been implicated in mitotic regulation, meiotic recombination control, DNA damage signaling, and autophagy in eukaryotes and in antiviral immunity in prokaryotes. Mechanistic parallels in HORMA-based signaling, as well as specialization in specific contexts, are emerging from efforts targeted at understanding how HORMA-based signaling acts in these diverse biological functions.

4.1. Bacterial Antiviral Immunity

While HORMA proteins and Pch2/TRIP13 are best understood in eukaryotic signaling, all eukaryotic HORMA proteins probably descended from a primordial bacterial protein that protects against infection by viruses (bacteriophages). Recent bioinformatics analyses have revealed a startling number and variety of bacterial immunity systems in addition to the well-known restriction-modification and CRISPR/Cas (clustered regularly interspaced short palindromic repeats/CRISPR-associated protein) systems (36, 37). In 2015, one such analysis identified a family of biosynthetic enzymes related to eukaryotic cyclic GMP–AMP synthase (cGAS), a mammalian innate-immune sensor that synthesizes a cyclic GMP–AMP second messenger molecule (10, 38, 39). Later work showed that these enzymes function in bacteriophage immunity: Phage infection is thought to activate synthesis of a cyclic di- or trinucleotide second messenger molecule, which in turn activates an effector protein encoded in the same operon that kills the cell to curtail viral replication. Overall, ∼10% of bacteria encode such a system, now collectively termed CBASS (cyclic oligonucleotide-based antiphage signaling system) (11, 40, 41).

Approximately 10% of CBASS operons encode one or two HORMA proteins and a TRIP13-like ATPase alongside the cGAS-related enzyme and effector protein (10, 42). In these systems, the HORMA proteins sense viral infection by binding a closure motif sequence in an unknown protein, either phage-derived or induced upon phage infection. The resulting HORMA–closure motif complex binds to its cognate cGAS-like enzyme, activating second messenger synthesis (**Figure 3**) (11, 43). HORMA-encoding CBASS systems fall into two classes, one of which encodes a single HORMA protein (termed HORMA1) and the other of which encodes two (HORMA2 and

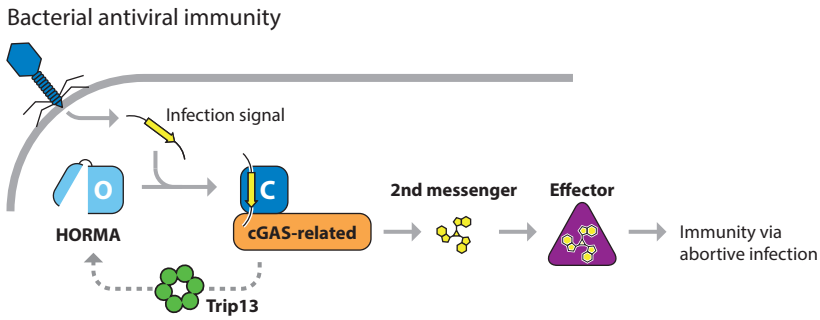

Figure 3

Roles of bacterial HORMA proteins in antiviral immunity. Functional schematic of a bacterial CBASS antiviral immunity pathway, with infection sensing through binding of a HORMA protein to an as-yet unidentified infection signal (*yellow*), followed by binding and activation of a cGAS-related enzyme to produce a nucleotide-based second messenger molecule. Second messenger production activates an effector enzyme to mediate immunity through a programmed-cell-death abortive infection mechanism (11, 40, 43). The role of Trip13 is unknown but may be to disassemble active signaling complexes (as pictured) or to maintain HORMA proteins in an open state poised for infection sensing (not shown) (11). Abbreviations: C, closed; CBASS, cyclic oligonucleotide-based antiphage signaling system; cGAS, cyclic GMP–AMP synthase; O, open.

HORMA3). In this second class, HORMA2 binds closure motif peptides and activates its cognate cGAS-like enzyme, while the role of HORMA3 is unknown (11). Phylogenetic analysis shows that eukaryotic HORMA and Pch2/TRIP13 proteins likely descended from bacterial HORMA2 proteins and their cognate Trip13 ATPases (26).

Many key questions remain with respect to the role of HORMA proteins and Trip13 in bacterial CBASS systems. First, what is the source of the activating closure motif? The HORMA proteins may directly recognize a viral protein, but such a mechanism would limit each CBASS system's response to a narrow class of bacteriophages. Another possibility is that the HORMA proteins piggyback on existing stress responses in their host cells, recognizing a host protein that is induced upon viral infection or sensing of a physiological change in the infected cell. Another open question concerns what role Trip13 plays in viral immunity. CBASS systems encoding HORMA proteins always also encode a Trip13-like ATPase, yet this protein is not required for antiviral immunity in a laboratory setting (11). In vitro, bacterial Trip13 recognizes the activated HORMA–cGAS complex and suppresses second messenger synthesis, likely through disassembly of the complex (**Figure 3**) (11). In cells, Trip13 may be required to maintain its cognate HORMA protein in an open conformation, poised to bind a closure motif and activate antiviral signaling. Related to this idea, Trip13 may also suppress spontaneous activation of CBASS signaling outside the context of an infection, thereby minimizing the toxicity of this cell-killing, or abortive infection, system. Ultimately, as described in Sections 4.2–4.4 for eukaryotic HORMA signaling pathways, optimal function of HORMA-containing CBASS systems likely relies on a delicate balance of HORMA–closure motif complex assembly and disassembly, closely monitored and regulated by Trip13.

4.2. Coordination of Mitotic Chromosome Segregation

In eukaryotes, proper genome segregation to daughter cells in mitosis requires that the kinetochores of replicated sister chromosomes each form bi-polar attachments to microtubules of the mitotic spindle (**Figure 4*a***). Chromosome segregation and mitotic exit are triggered by specific degradation of several proteins, mediated by a ubiquitin E3 ligase termed the anaphase promoting

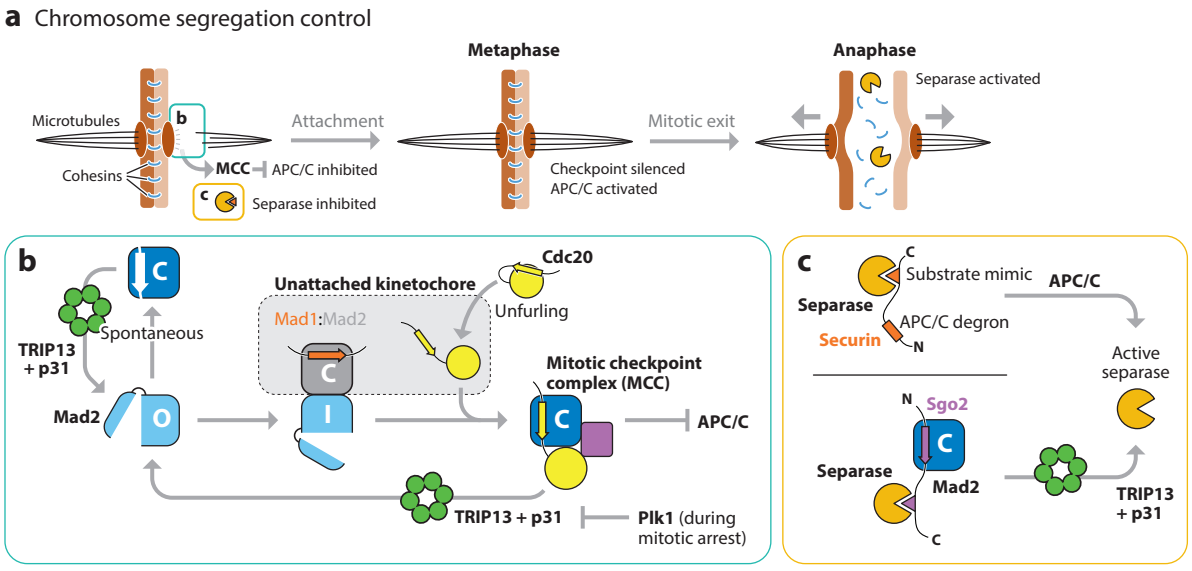

Figure 4

Roles of Mad2 in chromosome segregation control. (*a*) Schematic of mitotic chromosome segregation. (*Left*) Prior to kinetochore–microtubule attachment, unattached kinetochores generate a soluble MCC that binds and inhibits the APC/C (see panel *b*). Separase is inhibited by two substrate-analog inhibitors in mitotic prophase. (*Center*) After kinetochore–microtubule attachment is complete, MCC assembly ceases and the APC/C becomes activated to stimulate mitotic exit. (*Right*) Anaphase occurs upon cyclin B degradation (not shown) and separase activation, which leads to cleavage of cohesin complexes. (*b*) Assembly of Mad2–Cdc20 complexes at unattached kinetochores is the rate-limiting step of MCC assembly. After binding to kinetochore-localized Mad1–C-Mad2, O-Mad2 is converted to an intermediate (I) state primed for conversion to the closed state. At the same time, Cdc20 is recruited, and its closure motif is exposed for Mad2 binding followed by binding to BubR1–Bub3 (*purple square*) (59, 60). TRIP13 plays dual roles in Mad2 regulation: first to counteract spontaneous conversion of soluble O-Mad2 to an inactive closed/empty state and second to disassemble the MCC during spindle checkpoint silencing (22, 25). During mitosis, MCC disassembly is suppressed by Plk1-mediated phosphorylation of p31^{comet} (75, 76). (*c*) In checkpoint-active cells, separase is inhibited by two substrate mimics, including securin (*orange*) and a complex of Sgo2 (*purple*) and C-Mad2 (64). After checkpoint silencing, separase is activated by APC/C-mediated securin degradation and by TRIP13-mediated disassembly of Sgo2–Mad2 –separase complexes. Abbreviations: APC/C, anaphase promoting complex/cyclosome; C, closed; I, intermediate; MCC, mitotic checkpoint complex; O, open; Plk1, Polo-like kinase; Sgo2, shugoshin 2.

complex/cyclosome (APC/C) (44–46). To prevent chromosome segregation errors caused by premature mitotic exit, the SAC pathway monitors the status of kinetochore–microtubule attachment (47). Unattached kinetochores continually produce the MCC, which directly binds and inhibits the APC/C (48–51). Once all kinetochores have attached to spindle microtubules, MCC assembly ceases; subsequent degradation and active disassembly of the complex (described later in this section) allow APC/C activation, coordinated sister chromatid separation, and mitotic exit.

The MCC is composed of four proteins: Mad2, Cdc20, BubR1, and Bub3 (48). A recent biochemical reconstitution study showed that the rate-limiting step of MCC assembly is binding of Mad2 to a closure motif (also called a Mad2-interacting motif or MIM) in Cdc20 and that unattached kinetochores dramatically speed up Mad2–Cdc20 binding (51). The mechanistic basis for this speed-up involves several elements. First, a heterotetrameric complex of Mad1 and C-Mad2 is recruited to an unattached kinetochore (52–55). This Mad1–C-Mad2 complex in turn recruits soluble O-Mad2, which forms an asymmetric dimer with the Mad1-bound C-Mad2 (**Figure 2*b***) (27, 56). Dimerization with C-Mad2 introduces strain into the O-Mad2 protomer and promotes its conversion to the unbuckled transition state, priming it for closure motif

Anaphase promoting complex/cyclosome (APC/C): a 1.5-MDa ubiquitin E3 ligase that triggers chromosome segregation and mitotic exit

binding (30, 57, 58). In this manner, Mad2 acts as both a catalyst for MCC assembly (as part of the Mad1–Mad2 complex) and as a substrate. At the same time, Cdc20 is recruited to the kinetochore and unfurled to expose its Mad2-binding closure motif and position this motif precisely for Mad2 binding (59, 60). After binding, the resulting C-Mad2–Cdc20 complex spontaneously assembles with BubR1 and Bub3 to complete MCC assembly (**Figure 4*b***) (51, 59, 60).

In addition to promoting MCC formation as a means to coordinate chromosome segregation, Mad2 is implicated in control of a second key event at anaphase onset: the activation of the protease separase, which cleaves cohesin complexes holding sister chromatids together to initiate chromosome segregation (**Figure 4*a***) (61). Separase is inhibited prior to anaphase onset by securin and activated upon APC/C-mediated securin ubiquitination and degradation (62). Recently, a second, functionally redundant separase inhibitor has been identified in vertebrates, consisting of Mad2 bound to a closure motif in the shugoshin 2 (Sgo2) protein (63, 64). Mad2–Sgo2 binds separase as a substrate analog and prevents it from cleaving cohesin complexes, in a manner equivalent to securin (**Figure 4*c***). Assembly of Mad2–Sgo2 is proposed to occur at unattached kinetochores, although evidence for this proposal awaits future work. Nevertheless, Mad2–Sgo2 provides a distinct means to control separase activation and chromosome segregation independently of securin and the APC/C. Whether regulation of separase by Mad2 is as widely conserved as its role in the SAC is not yet clear, and this is important to assess in future work.

Mad2's dual roles in mitosis require a supply of soluble O-Mad2 that can be recruited to kinetochores and assembled with closure motifs on Cdc20 and Sgo2. Paradoxically, while cellular Mad2 exists mainly in the open conformation, purified O-Mad2 spontaneously converts to (empty) C-Mad2 with a half-life of only 1–2 hours (25, 65). To maintain cellular Mad2 in the open conformation, p31^{comet} specifically recognizes and binds C-Mad2 (5, 66) then recruits it to TRIP13 for conformational conversion (**Figures 2*d*,*e*** and **4*b***) (17–19, 23, 33, 67, 68). Without TRIP13 and p31^{comet}, cellular Mad2 rapidly converts to the closed conformation, making it impossible for cells to maintain sufficient O-Mad2 for SAC activation (22, 24, 25).

In addition to playing a key role in SAC activation through the maintenance of O-Mad2, p31^{comet} and TRIP13 also mediate SAC silencing and Mad2–Sgo2 complex disassembly after kinetochore–microtubule attachment (69–72). p31^{comet} can recognize C-Mad2 in the MCC and recruit it to TRIP13, where conformational conversion results in Cdc20 release and MCC disassembly (**Figure 4*b***) (19–21). Disassembly of Mad2–Sgo2 complexes through a similar mechanism causes dissociation of Sgo2 from separase, which (along with degradation of securin through APC/C-mediated ubiquitination) enables separase activation and cohesin cleavage to initiate chromosome segregation (**Figure 4*c***) (64). Thus, p31^{comet} and TRIP13 perform a single biochemical reaction that, depending on context, can contribute to either activation or silencing of HORMA-based signaling in mitosis (22, 25). As noted in Sections 4.3 and 4.4, more recent work has revealed that this functional paradigm also applies to Pch2/TRIP13's roles in meiotic regulation and likely also to Rev7-mediated DNA repair.

Given the dual roles of TRIP13 and p31^{comet} in the SAC, one question is whether these proteins are cell-cycle regulated. Both proteins are present and likely active throughout the cell cycle, although TRIP13 is upregulated in mitosis along with a core set of centromere and kinetochore proteins (17). p31^{comet} has been reported to be regulated by phosphorylation, but this is not yet well understood; in *Xenopus*, phosphorylation of p31^{comet} by IKK-β (inhibitor of nuclear factor κB kinase subunit β) appears to enhance Mad2 binding and promote SAC silencing (73). However, in human cells, p31^{comet} is phosphorylated by Plk1 (polo-like kinase 1) during mitosis, and this phosphorylation compromises p31^{comet}–Mad2 binding (74–76). Together with biochemical data showing that extracts from checkpoint-arrested cells show lower Mad2–Cdc20 disassembly activity than extracts from cycling cells (despite equivalent levels of p31^{comet} and TRIP13),

these data suggest that p31^{comet} phosphorylation suppresses p31^{comet}/TRIP13 activity specifically in mitosis (**Figure 4*b***) (76). Thus, PLK1-mediated regulation of p31^{comet} may enable cells to (*a*) maintain high levels of O-Mad2 in G2 as they approach mitosis, (*b*) inactivate p31^{comet} during checkpoint-mediated mitotic arrest to minimize MCC disassembly, and then (*c*) reactivate p31^{comet} upon checkpoint silencing to enable TRIP13-mediated MCC disassembly.

While Mad2's roles in coordinating chromosome segregation are well understood, Mad2 has also been reported to regulate key cell-cycle transitions in two other contexts. First, Mad2–Cdc20 complexes suppress APC/C activity in G2 to enable buildup of cyclin B, which is needed for cells to enter mitosis (77). Later, successful cytokinesis depends on Mad2 binding to a closure motif in the kinesin MKLP2, thus inhibiting MKLP2's association with the mitotic spindle (78). Independently of cell division, Mad2 and p31^{comet} have also been linked to control of insulin signaling; specifically, insulin receptor endocytosis was shown to be regulated by Mad2 binding to a closure motif in the insulin receptor's cytoplasmic C terminus (79, 80). Thus, Mad2 acts in several contexts outside of its canonical roles in chromosome segregation through its ability to undergo conformational conversion and engage closure motifs.

Homologous recombination (HR): double-strand break repair pathway that uses an unbroken template for error-free repair

4.3. Meiotic Recombination

Meiotic HORMA domain–containing proteins (HORMADs), including *S. cerevisiae* Hop1 and mammalian HORMAD1 and HORMAD2, are critical across eukaryotes for interhomolog recombination in meiosis. Meiosis is a specialized two-stage cell division program that produces haploid gametes from a diploid precursor cell and is therefore crucial for sexual reproduction in eukaryotes (81). Key to ploidy reduction is the recognition, physical association, and segregation of homologous chromosome pairs during meiosis I division, which is driven by a modified homologous recombination (HR) pathway between highly organized and linearly compacted chromosomes (**Figure 5*a***) (82–85). Early in meiotic prophase, HORMADs are recruited along the entire lengths of chromosomes by closure motifs in the filamentous chromosome axis core proteins (fungal Red1, plant ASY3, mammalian SYCP2) (**Figure 5*b***) (86–89), which in turn associate with meiosis-specific cohesin complexes to organize meiotic chromosomes as linear arrays of loops (82, 90–95). In mammals, HORMAD1 and HORMAD2 may be recruited through different mechanisms, with HORMAD2 binding the axis core protein SYCP2 (87) and HORMAD1 binding directly to meiotic cohesin complexes (96). Similarly, *Caenorhabditis elegans* lacks axis core proteins, and its four HORMADs form a hierarchical complex that likely binds directly to cohesin complexes (97–99). Once localized, HORMADs promote the formation of DNA breaks along each chromosome (100–104), likely by recruiting a conserved adapter complex termed RMM (Rec114, Mei4, Mer2/IHO1) (105–108), which in turn recruits the conserved DNA endonuclease Spo11 (**Figure 5*c***) (103, 108–110). Meiotic HORMADs also enforce a bias toward the use of the homolog—instead of the usually preferred sister chromosome—as a repair template, thereby promoting interhomolog interactions and recombination (111–114). In *S. cerevisiae*, this homolog bias is enforced through the activity of a kinase, Mek1, that is recruited to chromosomes through a direct interaction with phosphorylated Hop1 and locally inhibits the activity of recombination machinery, thereby suppressing sister-directed DNA repair (115–120).

Unique among HORMA proteins, meiotic HORMADs encode closure motifs in their own C termini. These motifs were first discovered in *C. elegans*, whose four meiotic HORMADs form a hierarchical assembly through specific HORMA domain–closure motif interactions (97). Discovery of similar motifs in the C termini of fungal, plant, and mammalian HORMADs suggested that they could also assemble head-to-tail oligomers at the chromosome axis, but experimental data supporting this model are lacking. More recent work has shown that meiotic HORMADs

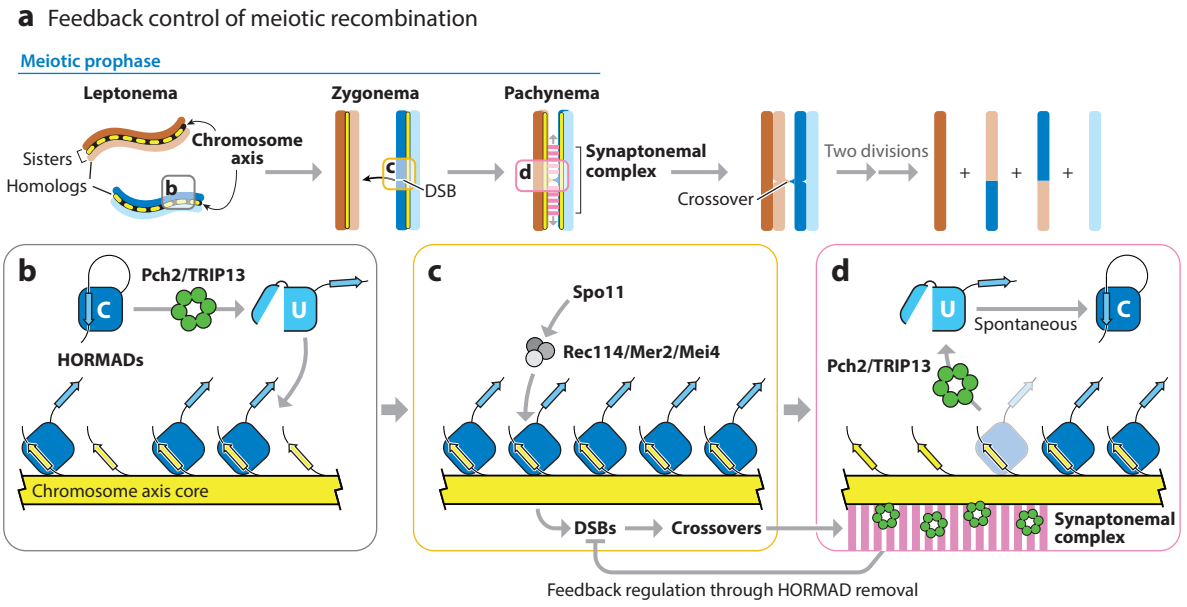

Figure 5

Feedback control of meiotic recombination by meiotic HORMAD proteins. (*a*) Schematic of eukaryotic meiosis. In early meiotic prophase (leptonema), replicated sister chromosome pairs (*dark/light brown* and *dark/light blue*) are organized and compacted by the chromosome axis (*yellow*) (see panel *b*). In leptonema/zygonema, axis-localized meiotic HORMAD proteins recruit Spo11 to generate DNA DSBs (see panel *c*). In zygonema/pachynema, invasion of the homologous chromosome and repair as an interhomolog crossover is coupled to assembly of the synaptonemal complex (*pink*) and removal of HORMADs from the axis (see panel *d*). Interhomolog crossovers enable alignment and segregation of homologs in meiosis I, followed by segregation of sister chromosomes in meiosis II to generate haploid gametes. (*b*) Early in meiotic prophase, soluble Pch2/TRIP13 catalyzes conversion of soluble self-closed HORMADs to the unbuckled (U) state, promoting their recruitment to closure motifs on meiotic chromosome axis core proteins (e.g., *S. cerevisiae* Red1, *M. musculus* SYCP2–SYCP3) (87, 121, 122). (*c*) Axis-localized HORMADs promote DNA DSB formation by recruiting the RMM (Rec114/Mei4/Mer2) complex (105), which in turn recruits the endonuclease Spo11. DSBs and recombination-mediated homologous chromosome engagement stimulates assembly of the synaptonemal complex between paired homologs. (*d*) Late in meiotic prophase, the assembled synaptonemal complex (*pink*) recruits Pch2/TRIP13, which catalyzes release of meiotic HORMADs to downregulate DNA breaks and crossovers (14, 16). Self-closure of the solubilized HORMADs likely prevents reassociation with the axis (86, 122). Abbreviations: C, closed; DSB, double-strand break; U, unbuckled.

Synaptonemal complex: a ladder-like protein complex with properties of biomolecular condensates that assembles between paired homologous chromosomes in meiotic prophase

can adopt a self-closed state with their HORMA domain bound to their own C-terminal closure motif (86). This state may be functionally analogous to O-Mad2, in that it represents a soluble, signaling-inactive state of the protein. In both fungi and plants, recruitment of HORMADs to the chromosome axis in early meiotic prophase is promoted by Pch2/TRIP13, suggesting that axis binding first requires conversion of the self-closed HORMAD protein to an unbuckled state (**Figure 5*b***) (86, 121–124). Not all organisms require Pch2/TRIP13 for HORMADs' initial recruitment to the axis; in these organisms, HORMADs' conformational equilibrium likely results in sufficient soluble, unbuckled HORMADs that are competent for axis association, such that early Pch2/TRIP13 activity is not needed (16, 125).

In most species, meiotic recombination drives the physical alignment and engagement of homologous chromosomes and is coupled to assembly of the synaptonemal complex, a ladder-like structure that physically links paired homologs' chromosome axes (82, 126, 127). Concomitant with synaptonemal complex assembly, the bulk of HORMADs are removed from the

chromosome axis through the action of Pch2/TRIP13, thereby downregulating further recombination on chromosomes that have successfully identified their homologs and formed crossovers (**Figure 5*d***) (14–16, 128–130). Thus, depending on meiotic prophase progression and its own localization, Pch2/TRIP13 can promote either assembly of meiotic HORMADs onto the chromosome axis or their removal from the axis. Further, self-closure of meiotic HORMADs likely serves an important regulatory role in preventing excess double-strand break (DSB) formation by preventing promiscuous binding of HORMADs to the chromosome axis either before or after their activity is required.

How meiotic HORMADs are recognized by Pch2/TRIP13 remains an important unresolved question. In plants, there is compelling evidence that the Mad2 adapter p31^{comet} is associated with the synaptonemal complex in late meiotic prophase and that it plays a role in PCH2-mediated remodeling of the meiotic HORMAD protein ASY1 (131, 132). P31^{comet}'s involvement in meiotic HORMAD regulation is not, however, universal. Comparative genomics has shown that organisms tend to encode Pch2/TRIP13 if either p31^{comet} or meiotic HORMADs are also present (cooccurrence value 0.766, with 1.0 representing perfect cooccurrence), which is unsurprising given Pch2/TRIP13's role in regulation of both Mad2 and meiotic HORMADs (133). At the same time, p31^{comet} and meiotic HORMADs show low evolutionary correlation (cooccurrence value 0.162), suggesting that they are functionally uncoupled in most organisms. Indeed, p31^{comet} is absent in the budding yeast *S. cerevisiae*, in which Pch2's role in meiotic HORMAD regulation was discovered (13, 14). How, then, are meiotic HORMADs recognized by Pch2/TRIP13? One possibility is that HORMADs are recognized directly, perhaps forming a homodimer analogous to the Mad2–p31^{comet} heterodimer, in which one protomer mediates Pch2/TRIP13 binding, and the other serves as the substrate. This idea is supported by reports that in *S. cerevisiae*, which lacks p31^{comet}, Pch2 binds directly to Hop1 (134, 135). Alternatively, an as-yet-unidentified protein may serve as an adapter in this pathway. Finally, Pch2/TRIP13 may engage the disordered N terminus of meiotic HORMADs directly, bypassing the need for an adapter protein. Resolving this question remains an important area for future study.

Double-strand break (DSB): DNA damage resulting from exogenous insults, DNA replication errors, or (in meiosis) activation of the Spo11 endonuclease

Translesion DNA synthesis (TLS): DNA damage repair pathway that bypasses replication-stalling lesions using specialized inserter and extender DNA polymerases

4.4. Regulation of DNA Repair by Rev7

Rev7 (also called MAD2B or MAD2L2) acts as a key scaffolding factor in two important DNA damage repair pathways. Rev7 was initially described as a component of the DNA polymerase zeta (Polζ) complex, which cooperates with other repair polymerases to bypass DNA lesions that stall replicative polymerases (**Figure 6*a***) (136–140). The Polζ catalytic subunit Rev3 contains a large insertion in its polymerase domain that encodes two closure motifs, also termed Rev7-binding motifs (RBMs) (141–143). Biochemical studies and structures of subcomplexes suggested that these RBMs bind two copies of Rev7, which form a homodimer in the Polζ complex (142, 144). This model was recently confirmed by high-resolution structures of the Polζ holoenzyme from the budding yeast *S. cerevisiae* (145, 146). These structures confirmed that Rev3 binds two copies of Rev7 through its two RBMs and revealed that the two Rev7 protomers form a head-to-tail homodimer distinct from other HORMA domain dimer structures (**Figure 6*b***). Rev7 is not directly involved in catalysis but rather coordinates translesion DNA synthesis (TLS) by assembling multi-polymerase complexes. Rev3-bound Rev7 can bind directly to the C-terminal domain of the Y-family polymerase Rev1, which in turn binds other Y-family polymerases including Polη, Polι, and Polκ (147–150). In translesion synthesis, these Y-family inserter polymerases can introduce a nucleotide opposite a lesion in the template strand. Rev3/Polζ extends this nascent strand and eventually hands off to a replicative polymerase to continue DNA synthesis (**Figure 6*a***) (151, 152).

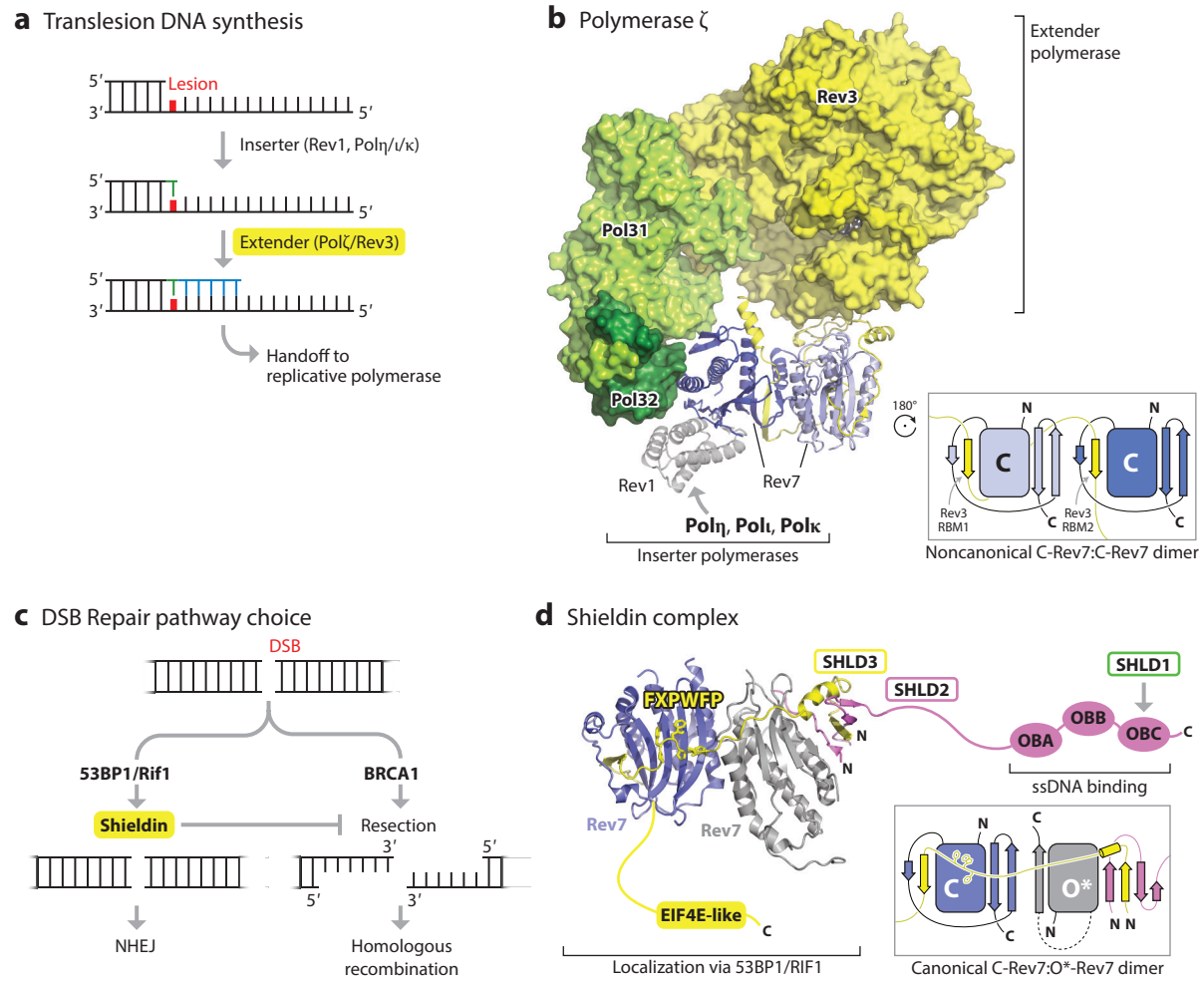

Figure 6

Architecture and function of Rev7 DNA repair complexes. (*a*) Schematic of translesion DNA synthesis mediated by coordinated activity of Y-family inserter polymerases (Rev1, Polη, Polι, and Polκ), and the extender polymerase Polζ (catalytic subunit: Rev3). (*b*) Structure of the polymerase ζ holoenzyme, with catalytic Rev3 subunit in yellow, accessory subunits Pol31 and Pol32 in light and dark green, respectively, and two copies of Rev7 colored light and dark blue [PDB ID: 6V93 (145)]. The C-terminal domain of Rev1 (*gray*) is modeled based on a separate structure of Rev7 bound to a single Rev3 RBM and Rev1 [PDB ID: 4GK5 (232)]. (*Inset*) Conformation of the noncanonical C-Rev7–C-Rev7 dimer bound to Rev3 RBM1 and RBM2. (*c*) Schematic of DNA double-strand break repair pathway choice. Shieldin is recruited to broken DNA ends by 53BP1/Rif1 and then inhibits end resection to suppress homologous recombination and promote nonhomologous end joining. (*d*) Structure of the shieldin core complex, containing a C-Rev7–O*-Rev7 dimer (*blue* and *gray*, respectively), SHLD2 (*pink*), and SHLD3 (*yellow*). SHLD1 is thought to associate with the OB domains of SHLD2 (233). The conserved FXPWFP motif of SHLD3 is shown as sticks [PDB ID: 6KTO (29)]. (*Inset*) Conformation of the C-Rev7–O*-Rev7 dimer bound to SHLD2 and SHLD3. Abbreviations: C, closed; DSB, double-strand break; NHEJ, nonhomologous end joining; O, open; OB, oligonucleotide/oligosaccharide-binding; Pol, polymerase.

In 2015, Rev7 was reported to regulate pathway choice in the repair of DNA DSBs (153). DSBs present a huge threat to genome stability and are repaired either through the high-fidelity HR pathway or the error-prone nonhomologous end joining (NHEJ) pathway. In vertebrates, Rev7 nucleates a complex named shieldin that is recruited to DSB sites by 53BP1–RIF1 and inhibits

resection of broken DNA ends, thereby suppressing repair by HR and promoting NHEJ (**Figure 6*c***) (154–157). Rev7 is the central scaffold that brings together SHLD3, which mediates binding to 53BP1–RIF1, and SHLD2, whose single-stranded DNA–binding activity is required for inhibition of DSB resection (158). A recent structure of the Rev7–SHLD2 –SHDL3 complex (29) revealed a Rev7 dimer similar to the C-Mad2–O-Mad2 dimer, with one protomer adopting the closed state around an RBM in SHLD3 and the other adopting a noncanonical open state stabilized by SHLD2 and SHLD3 (**Figure 6*d***). Thus, an asymmetric Rev7 dimer acts as a bridge to connect shieldin's recruitment subunit, SHLD3, to its DNA-binding subunit, SHLD2. The Rev7 dimers found in Polζ and shieldin are strikingly different, illustrating the structural plasticity of the HORMA domain, and Rev7 in particular, for scaffolding assembly of multi-protein signaling complexes.

Nonhomologous end joining (NHEJ): error-prone double-strand break repair pathway that fuses broken DNA ends nonspecifically

Rev7 is the closest eukaryotic relative of Mad2, and in keeping with this relationship, recent findings have revealed that the Mad2 regulators p31^{comet} and TRIP13 also regulate Rev7. Purified Rev7 adopts two different conformations in solution, paralleling earlier findings with Mad2, and TRIP13 can disassemble Rev7–SHLD3 complexes in vitro and control the relative levels of complexed versus monomeric Rev7 in cells (12). In an additional parallel with Mad2, p31^{comet} is also involved in TRIP13-dependent Rev7 regulation (159). Moreover, both TRIP13 and p31^{comet} promote HR-mediated DSB repair, presumably by disassembling and inactivating Rev7-containing shieldin complexes (12, 159). These findings further cement the mechanistic parallels between the three major families of eukaryotic HORMA proteins and raise interesting questions about how TRIP13 and p31^{comet} regulate the levels of translesion polymerase and shieldin complexes, for example, during cell-cycle progression or in response to DNA-damaging agents.

Outside of DNA repair, Rev7 has been reported to interact with a number of additional proteins including the cell-cycle regulator Cdh1/FZR1 (160–162); the small GTPase Ran (163, 164); chromosome alignment maintaining phosphoprotein (165); and a *Shigella* invasin protein, IpaB (164, 166). These data imply that Rev7 may have additional important signaling roles in cells; however, these roles are not yet well defined.

4.5. Autophagy

In addition to their diverse roles in genome maintenance, HORMA proteins play key roles in the initiation of autophagy, the cellular process that removes superfluous or damaged cytoplasmic contents in eukaryotic cells (167). During autophagy, cytoplasmic contents are engulfed by a double-membrane-bound autophagosome, which eventually fuses with the lysosome for digestion (**Figure 7*a***). Autophagy is initiated when the kinase activity of the TOR complex (mTORC1) is suppressed by starvation, leading to dephosphorylation of the HORMA protein Atg13 (168–170). Atg13 possesses an N-terminal HORMA domain and an extended C-terminal region that binds the ULK1 kinase (Atg1 in budding yeast) (171); the molecular scaffold FIP200 (Atg17–29–31 in budding yeast) (171–173); and in budding yeast, the vacuolar protein Vac8 (174, 175). Multivalent interactions between Atg13 and FIP200/Atg17 are triggered by Atg13 dephosphorylation and have been shown to induce liquid–liquid phase separation to drive assembly of the PAS (phagophore assembly site) (**Figure 7*b***) (172, 176, 177). The PAS then recruits additional proteins and lipid vesicles to assemble the phagophore, which expands around the cell contents to be degraded and seals into a double membrane-bound compartment, completing autophagosome assembly.

In *Schizosaccharomyces pombe* and mammals, Atg13 forms a canonical HORMA–HORMA dimer with Atg13 in the closed conformation and Atg101 in a modified open conformation (**Figures 1*b*** and **7*c***) (7, 9). The Atg13–Atg101 dimer is thought to mediate recruitment of additional downstream autophagy factors to the PAS, at least in part through unique structural elements like the

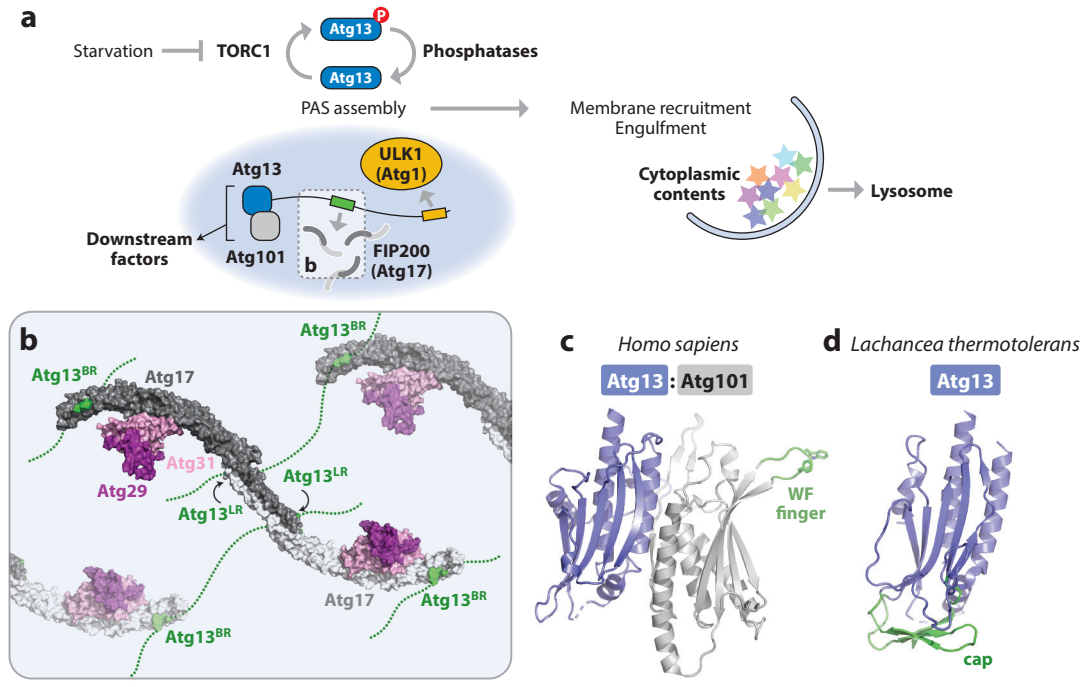

Figure 7

Role of Atg13 in autophagy initiation. (*a*) Autophagy is initiated when starvation suppresses TORC1 kinase activity, leading to dephosphorylation of Atg13. Dephosphorylated Atg13 serves as an assembly hub for the PAS, by binding multiple partners including ULK1 (Atg1) (*orange*) (171), FIP200 (Atg17) (*gray*) (171–173), and Vac8 (budding-yeast specific; not shown) (174). The Atg13 HORMA domain binds Atg101 (missing in budding yeast) and additional downstream factors including Atg9 and Atg14 (6, 7, 9, 181). (*b*) Structure of the budding yeast Atg17–Atg29–Atg31 complex (*gray*, *purple*, and *pink*, respectively) with Atg13's Atg17-linking region (residues 359–389) and Atg17-binding region (residues 424–436) (*green*) [PDB ID: 5JHF (172)]. Dotted lines schematize multivalent binding of Atg17 complexes and Atg13, which leads to phase separation (176). (*c*) Structure of the *Homo sapiens* Atg13–Atg101 HORMA domain dimer, with Atg13 shown in blue and Atg101 in gray. The WF finger, a loop encoding conserved tryptophan (W) and phenylalanine (F) residues, is shown in green [PDB ID: 5XV4 (28)]. (*d*) Structure of the budding yeast Atg13 HORMA domain (*Lachancea thermotolerans*; 50% identical to *Saccharomyces cerevisiae* Atg13 in this domain), with cap domain in green [PDB ID: 4J2G (6)]. Abbreviations: PAS, phagophore assembly site; PDB ID, Protein Data Bank identifier.

WF finger in Atg101 (6, 7, 9, 172, 178–180). Budding yeast lack Atg101, and in these organisms, Atg13's closed conformation appears to be stabilized by an insertion in the HORMA domain termed the cap (**Figure 7*d***) (6). The HORMA domain of budding yeast Atg13 has been implicated in binding the cytoplasmic vesicle-associated protein Atg9 (181, 182) and also recruits Atg14, a subunit of the phosphatidylinositol 3-kinase complex (6). The structural basis of these interactions has not been determined, leaving open the question of whether Atg13 recruits downstream factors through canonical HORMA–closure motif interactions.

Both Atg13 and Atg101 show high divergence from the more closely related Mad2, Rev7, and meiotic HORMAD proteins. Whether Atg13 and Atg101 share their relatives' ability to undergo dynamic conformational changes and form complexes in response to cellular signals is currently unknown (180). It is also unknown whether Atg13 and/or Atg101 are regulated by Pch2/TRIP13. Given the importance of autophagy for homeostasis in all eukaryotic cells, and the central organizing role for Atg13 and Atg101 in autophagy initiation, addressing how these proteins' HORMA domains contribute to autophagy initiation and regulation is an important area for future study.

5. HORMA PROTEINS AND TRIP13 IN CANCER

Cancer is characterized by uncontrolled cell growth and proliferation. While the disease is highly heterogeneous, many cancers display misregulation of particular DNA repair pathways and increased chromosomal instability and aneuploidy (183). HORMA proteins, and especially their regulators TRIP13 and p31^{comet}, stand at the crossroads of chromosome segregation and DNA repair, and as such, they have become increasingly recognized as key players in many cancers.

PARP inhibitor: a chemical inhibitor of poly ADP ribose polymerase (PARP) that targets HR-deficient tumors by inhibiting PARP-dependent DNA repair

A major feature of cancer genomes is aneuploidy, which can arise through chromosome segregation errors in cells with a dysfunctional SAC. Many cancers show altered expression of SAC proteins including Mad2 (184) and TRIP13, but it remains unclear whether defects in Mad2 or other SAC proteins contribute to cancer onset or progression. Many cancers also show high expression of meiotic HORMAD proteins, whose expression is normally restricted to the germline (185–195). HORMAD1 overexpression in cancer cells is correlated with genome instability (191) and altered responses to DNA-damaging agents and inhibitors of the DNA repair protein poly-ADP ribose polymerase (PARP) (187, 188, 191, 193), suggesting a direct link between HORMAD1 expression and dysregulation of DNA DSB repair. Other studies have found that HORMAD1 overexpression compromises additional DNA repair pathways, including DNA mismatch repair (196). The mechanistic basis for these effects, and their ultimate contribution to the onset and progression of cancer, remains poorly understood.

In contrast to Mad2 and the meiotic HORMADs, the mechanistic linkage of Rev7 and the shieldin complex to cancer is clearer. The first studies hinting at the existence of the shieldin complex found that loss of Rev7 restores HR in tumors that have lost the ability to perform HR due to mutation or loss of BRCA1 (153, 197). This observation was explained by the realization that loss of Rev7 in these tumors compromised the activity of the shieldin complex, reactivating HR-mediated DNA break repair independently of BRCA1. These findings have provided an explanation for why loss of Rev7 confers resistance to a class of anticancer drugs called PARP inhibitors that target BRCA1-deficient cancer cells (153–157, 198). Rev7's role in TLS also influences the progression of cancers and their response to therapeutic agents: Loss of Rev7 or inhibition of TLS suppresses tumor growth and increases sensitivity to the DNA-damaging agent cisplatin (143, 199–201). Thus, by regulating the balance between HR and NHEJ via shieldin and acting in TLS via scaffolding of Polζ, Rev7 plays an important role in cancer progression and dictates how tumors respond to therapeutic agents that target specific DNA repair pathways in cancer cells.

While Rev7 plays a role in specific cancer contexts, it is becoming increasingly clear that misregulation of the HORMA regulator TRIP13 is a much more common feature of cancers. Long before its function as a universal HORMA regulator was clarified, TRIP13 was identified as a highly expressed gene in undifferentiated cancers (202) whose overexpression strongly correlates with chromosomal instability and aneuploidy (203). More recently, individual studies have linked TRIP13 overexpression and/or copy number amplification to cancers of the liver (204–207), breast (204, 208–210), lung (204, 211–213), colon (214–216), and many other tissues (217–229). Data from The Cancer Genome Atlas show that, in some cancer types, up to 40% of patients show genomic copy number amplification of TRIP13 or p31^{comet} (**Supplemental Figure 2*a***). Increased copy number and expression of TRIP13 are both strongly correlated with poor prognosis across cancers (**Supplemental Figure 2*b*,*c***). Consistent with these correlations, experiments in cancer cells have shown that TRIP13 overexpression increases proliferation and metastasis phenotypes, and knockdown or inhibition of TRIP13 inhibits these phenotypes, increases apoptosis, and reduces tumor load (205, 212, 213, 215, 219, 220, 228, 230). Recently, the first reported

Supplemental Material >

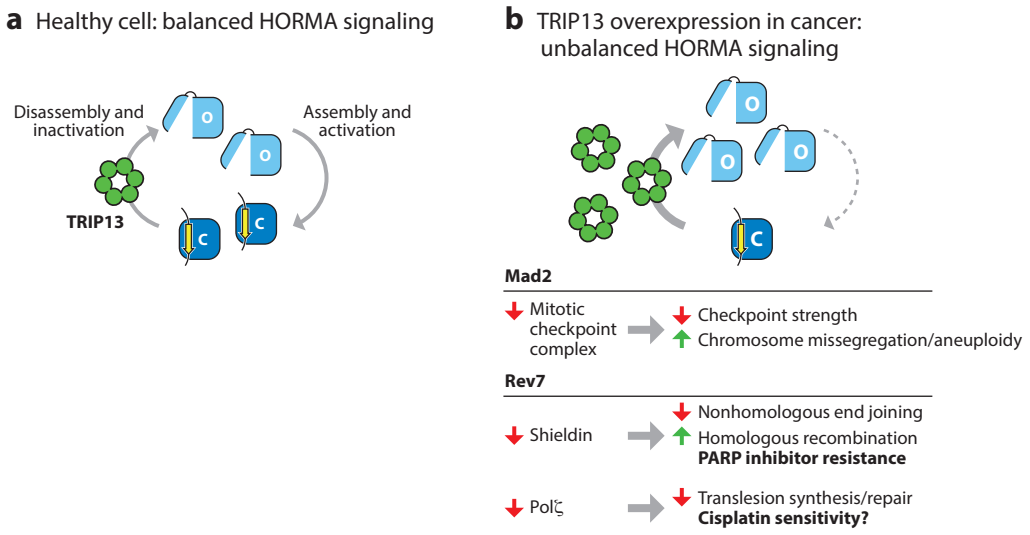

Figure 8

Consequences of TRIP13 misregulation in cancer. (*a*) Generalized schematic of HORMA protein signaling in healthy cells, with balanced assembly and disassembly kinetics. (*b*) Schematic of unbalanced HORMA protein signaling upon TRIP13/p31^{comet} overexpression, as observed in a large fraction of cancers (**Supplemental Figure 2**). TRIP13-mediated mitotic checkpoint complex disassembly can weaken the spindle assembly checkpoint and increase cell proliferation (234). Similarly, TRIP13-mediated disassembly of Rev7 complexes affects cancer cells in multiple ways: Reduced shieldin complex levels promote homologous recombination and can lead to PARP inhibitor resistance, while reduced Polymerase ξ levels may impair translesion DNA synthesis and promote sensitivity to DNA-damaging agents like cisplatin. Abbreviations: C, closed; O, open; PARP, poly-ADP ribose polymerase; Pol, polymerase.

Supplemental Material >

small-molecule inhibitor of TRIP13 was shown to reduce proliferation in multiple myeloma, highlighting the potential for TRIP13 inhibition as a broadly applicable cancer treatment (229).

How does TRIP13 overexpression drive cancer? Proper function of Mad2 in coordinating chromosome segregation and Rev7 in DNA repair each depend on a balance between assembly and disassembly of HORMA protein–closure motif complexes mediated by TRIP13 and its adapter p31^{comet} (**Figure 8*a***). Overexpression of one or both of these proteins in cancers may disrupt this balance, driving disassembly of signaling complexes and compromising chromosome segregation and DNA repair fidelity (**Figure 8*b***). Indeed, TRIP13 overexpression mediates resistance to the PARP inhibitor Olaparib in *BRCA1*-deficient cancer cells, likely because TRIP13 overexpression inhibits the shieldin complex, enabling these previously HR-deficient cells to reactivate HR (12). At the same time, lower levels of active Polξ in cells overexpressing TRIP13 may lead to a defect in translesion DNA repair and sensitivity to cisplatin and other DNA-damaging agents, as seen in cells lacking Rev7 (143, 199–201). Finally, complete loss of TRIP13 is also harmful, predisposing patients to Wilms Tumor, mosaic aneuploidies, and high levels of chromosome mis-segregation (231). These findings are reminiscent of the fairy-tale situation of Goldilocks, since either too much or too little TRIP13 activity is harmful and avoiding cancer onset and progression requires that TRIP13 levels be just right.

6. CONCLUSION

In the two decades since their discovery in 1998, our understanding of HORMA domains and their roles in cellular signaling across kingdoms has grown remarkably. We now understand the HORMA domain as a general-purpose protein complex scaffold, whose closure motif–bound

closed conformation serves as a platform for assembly of larger signaling and enzymatic complexes. The topologically linked nature of a HORMA domain–closure motif complex lends it uncommon stability, which is likely advantageous in the diverse pathways in which proteins with this domain act. The unique energy landscape of the HORMA domain explains why it has evolved alongside a dedicated AAA+ ATPase regulator, Pch2/TRIP13, which is required to disassemble HORMA–closure motif complexes and maintain the high-energy open conformation that is poised for closure motif binding. Our deep mechanistic knowledge of the HORMA domain–Pch2/TRIP13 signaling module now sets the stage for interventions, notably including the development of TRIP13-targeting therapeutics that may be useful in the fight against cancer.

SUMMARY POINTS

1. HORMA domain proteins are a conserved family of signaling proteins that originated in bacteria, and in eukaryotes has expanded to play key roles in several chromosome maintenance, cell cycle, sexual reproduction, and cellular homeostasis pathways.
2. The HORMA domain assembles signaling complexes by binding closure motif sequences to binding partners through a distinctive safety belt mechanism.
3. HORMA domain–closure motif binding is regulated by conformational switching between an unbound open state and a closed state that forms a topologically linked complex with a closure motif.
4. HORMA domain–closure motif complexes scaffold important signaling complexes in the spindle assembly checkpoint, DNA repair, meiotic recombination, and autophagy pathways.
5. The AAA+ ATPase Pch2/TRIP13 is a near-universal regulator of HORMA proteins whose conformational conversion activity is required for both activation and inactivation of signaling.
6. The multiple roles of TRIP13 in genome maintenance explain its high frequency of overexpression in cancer and highlight it as a novel therapeutic target.

DISCLOSURE STATEMENT

The authors are not aware of any affiliations, memberships, funding, or financial holdings that might be perceived as affecting the objectivity of this review.

ACKNOWLEDGMENTS

The authors thank members of the Corbett and Desai labs for helpful discussions and A. D'Andrea, A. Schnittger, and A. Musacchio for sharing results prior to publication.

LITERATURE CITED

1. Aravind L, Koonin EV. 1998. The HORMA domain: a common structural denominator in mitotic checkpoints, chromosome synapsis and DNA repair. *Trends Biochem. Sci.* 23:284–86
2. Mapelli M, Musacchio A. 2007. MAD contortions: Conformational dimerization boosts spindle checkpoint signaling. *Curr. Opin. Struct. Biol.* 17:716–25
3. Skinner JJ, Wood S, Shorter J, Englander SW, Black BE. 2008. The Mad2 partial unfolding model: regulating mitosis through Mad2 conformational switching. *J. Cell Biol.* 183:761–68

4. Luo X, Yu H. 2008. Protein metamorphosis: the two-state behavior of Mad2. *Structure* 16:1616–25
5. Yang M, Li B, Tomchick DR, Machius M, Rizo J, et al. 2007. p31^{comet} blocks Mad2 activation through structural mimicry. *Cell* 131:744–55
6. Jao CC, Ragusa MJ, Stanley RE, Hurley JH. 2013. A HORMA domain in Atg13 mediates PI 3-kinase recruitment in autophagy. *PNAS* 110:5486–91
7. Suzuki H, Kaizuka T, Mizushima N, Noda NN. 2015. Structure of the Atg101–Atg13 complex reveals essential roles of Atg101 in autophagy initiation. *Nat. Struct. Mol. Biol.* 22:572–80
8. Hegedus K, Nagy P, Gaspari Z, Juhasz G. 2014. The putative HORMA domain protein Atg101 dimerizes and is required for starvation-induced and selective autophagy in *Drosophila*. *Biomed. Res. Int.* 2014:470482
9. Qi S, Kim DJ, Stjepanovic G, Hurley JH. 2015. Structure of the human Atg13–Atg101 HORMA heterodimer: an interaction hub within the ULK1 complex. *Structure* 23:1848–57
10. Burroughs AM, Zhang D, Schaffer DE, Iyer LM, Aravind L. 2015. Comparative genomic analyses reveal a vast, novel network of nucleotide-centric systems in biological conflicts, immunity and signaling. *Nucleic Acids Res.* 43:10633–54
11. Ye Q, Lau RK, Mathews IT, Birkholz EA, Watrous JD, et al. 2020. HORMA Domain proteins and a Trip13-like ATPase regulate bacterial cGAS-like enzymes to mediate bacteriophage immunity. *Mol. Cell* 77:709–22.e7
12. Clairmont CS, Sarangi P, Ponnienselvan K, Galli LD, Csete I, et al. 2020. TRIP13 regulates DNA repair pathway choice through REV7 conformational change. *Nat. Cell. Biol.* 22:87–96
13. San-Segundo PA, Roeder GS. 1999. Pch2 links chromatin silencing to meiotic checkpoint control. *Cell* 97:313–24
14. Borner GV, Barot A, Kleckner N. 2008. Yeast Pch2 promotes domainal axis organization, timely recombination progression, and arrest of defective recombinosomes during meiosis. *PNAS* 105:3327–32
15. Joshi N, Barot A, Jamison C, Borner GV. 2009. Pch2 links chromosome axis remodeling at future crossover sites and crossover distribution during yeast meiosis. *PLOS Genet.* 5:e1000557
16. Wojtasz L, Daniel K, Roig I, Bolcun-Filas E, Xu H, et al. 2009. Mouse HORMAD1 and HORMAD2, two conserved meiotic chromosomal proteins, are depleted from synapsed chromosome axes with the help of TRIP13 AAA-ATPase. *PLOS Genet.* 5:e1000702
17. Tipton AR, Wang K, Oladimeji P, Sufi S, Gu Z, Liu ST. 2012. Identification of novel mitosis regulators through data mining with human centromere/kinetochore proteins as group queries. *BMC Cell Biol.* 13:15
18. Wang K, Sturt-Gillespie B, Hittle JC, Macdonald D, Chan GK, et al. 2014. Thyroid hormone receptor interacting protein 13 (TRIP13) AAA-ATPase is a novel mitotic checkpoint-silencing protein. *J. Biol. Chem.* 289:23928–37
19. Ye Q, Rosenberg SC, Moeller A, Speir JA, Su TY, Corbett KD. 2015. TRIP13 is a protein-remodeling AAA+ ATPase that catalyzes MAD2 conformation switching. *eLife* 4:e07367
20. Eytan E, Wang K, Miniowitz-Shemtov S, Sitry-Shevah D, Kaisari S, et al. 2014. Disassembly of mitotic checkpoint complexes by the joint action of the AAA-ATPase TRIP13 and p31^{comet}. *PNAS* 111:12019–24
21. Miniowitz-Shemtov S, Eytan E, Kaisari S, Sitry-Shevah D, Hershko A. 2015. Mode of interaction of TRIP13 AAA-ATPase with the Mad2-binding protein p31^{comet} and with mitotic checkpoint complexes. *PNAS* 112:11536–40
22. Ma HT, Poon RYC. 2016. TRIP13 regulates both the activation and inactivation of the spindle-assembly checkpoint. *Cell Rep.* 14:1086–99
23. Ye Q, Kim DH, Dereli I, Rosenberg SC, Hagemann G, et al. 2017. The AAA+ ATPase TRIP13 remodels HORMA domains through N-terminal engagement and unfolding. *EMBO J.* 36:2419–34
24. Ma HT, Poon RYC. 2018. TRIP13 functions in the establishment of the spindle assembly checkpoint by replenishing O-MAD2. *Cell Rep.* 22:1439–50
25. Kim DH, Han JS, Ly P, Ye Q, McMahon MA, et al. 2018. TRIP13 and APC15 drive mitotic exit by turnover of interphase- and unattached kinetochore-produced MCC. *Nat. Commun.* 9:4354
26. Tromer EC, van Hooff JJE, Kops G, Snel B. 2019. Mosaic origin of the eukaryotic kinetochore. *PNAS* 116:12873–82

27. Mapelli M, Massimiliano L, Santaguida S, Musacchio A. 2007. The Mad2 conformational dimer: structure and implications for the spindle assembly checkpoint. *Cell* 131:730–43
28. Kim BW, Jin Y, Kim J, Kim JH, Jung J, et al. 2018. The C-terminal region of ATG101 bridges ULK1 and PtdIns3K complex in autophagy initiation. *Autophagy* 14:2104–16
29. Liang L, Feng J, Zuo P, Yang J, Lu Y, Yin Y. 2020. Molecular basis for assembly of the shieldin complex and its implications for NHEJ. *Nat. Commun.* 11:1972
30. Hara M, Ozkan E, Sun H, Yu H, Luo X. 2015. Structure of an intermediate conformer of the spindle checkpoint protein Mad2. *PNAS* 112:11252–57
31. Puchades C, Sandate CR, Lander GC. 2020. The molecular principles governing the activity and functional diversity of AAA+ proteins. *Nat. Rev. Mol. Cell Biol.* 21:43–58
32. Sauer RT, Baker TA. 2011. AAA+ proteases: ATP-fueled machines of protein destruction. *Annu. Rev. Biochem.* 80:587–612
33. Alfieri C, Chang L, Barford D. 2018. Mechanism for remodelling of the cell cycle checkpoint protein MAD2 by the ATPase TRIP13. *Nature* 559:274–78
34. Brulotte ML, Jeong BC, Li F, Li B, Yu EB, et al. 2017. Mechanistic insight into TRIP13-catalyzed Mad2 structural transition and spindle checkpoint silencing. *Nat. Commun.* 8:1956
35. Xie W, Wang S, Wang J, de la Cruz MJ, Xu G, et al. 2021. Molecular mechanisms of assembly and TRIP13-mediated remodeling of the human Shieldin complex. *PNAS* 118:e2024512118
36. Doron S, Melamed S, Ofir G, Leavitt A, Lopatina A, et al. 2018. Systematic discovery of antiphage defense systems in the microbial pangenome. *Science* 359:eaar4120
37. Gao L, Altae-Tran H, Bohning F, Makarova KS, Segel M, et al. 2020. Diverse enzymatic activities mediate antiviral immunity in prokaryotes. *Science* 369:1077–84
38. Wu J, Chen ZJ. 2014. Innate immune sensing and signaling of cytosolic nucleic acids. *Annu. Rev. Immunol.* 32:461–88
39. Davies BW, Bogard RW, Young TS, Mekalanos JJ. 2012. Coordinated regulation of accessory genetic elements produces cyclic di-nucleotides for *V. cholerae* virulence. *Cell* 149:358–70
40. Cohen D, Melamed S, Millman A, Shulman G, Oppenheimer-Shaanan Y, et al. 2019. Cyclic GMP-AMP signalling protects bacteria against viral infection. *Nature* 574:691–95
41. Whiteley AT, Eaglesham JB, de Oliveira Mann CC, Morehouse BR, Lowey B, et al. 2019. Bacterial cGAS-like enzymes synthesize diverse nucleotide signals. *Nature* 567:194–99
42. Millman A, Melamed S, Amitai G, Sorek R. 2020. Diversity and classification of cyclic-oligonucleotide-based anti-phage signalling systems. *Nat. Microbiol.* 5:1608–15
43. Lau RK, Ye Q, Birkholz EA, Berg KR, Patel L, et al. 2020. Structure and mechanism of a cyclic trinucleotide-activated bacterial endonuclease mediating bacteriophage immunity. *Mol. Cell* 77:723–33.e6
44. Primorac I, Musacchio A. 2013. Panta rhei: the APC/C at steady state. *J. Cell Biol.* 201:177–89
45. King RW, Peters JM, Tugendreich S, Rolfe M, Hieter P, Kirschner MW. 1995. A 20S complex containing CDC27 and CDC16 catalyzes the mitosis-specific conjugation of ubiquitin to cyclin B. *Cell* 81:279–88
46. Sudakin V, Ganoth D, Dahan A, Heller H, Hershko J, et al. 1995. The cyclosome, a large complex containing cyclin-selective ubiquitin ligase activity, targets cyclins for destruction at the end of mitosis. *Mol. Biol. Cell* 6:185–97
47. Musacchio A. 2015. The molecular biology of spindle assembly checkpoint signaling dynamics. *Curr. Biol.* 25:R1002–18
48. Sudakin V, Chan GK, Yen TJ. 2001. Checkpoint inhibition of the APC/C in HeLa cells is mediated by a complex of BUBR1, BUB3, CDC20, and MAD2. *J. Cell Biol.* 154:925–36
49. Kulukian A, Han JS, Cleveland DW. 2009. Unattached kinetochores catalyze production of an anaphase inhibitor that requires a Mad2 template to prime Cdc20 for BubR1 binding. *Dev. Cell* 16:105–17
50. Corbett KD. 2017. Molecular mechanisms of spindle assembly checkpoint activation and silencing. *Prog. Mol. Subcell. Biol.* 56:429–55
51. Faesen AC, Thanasoula M, Maffini S, Breit C, Muller F, et al. 2017. Basis of catalytic assembly of the mitotic checkpoint complex. *Nature* 542:498–502

52. Chen RH, Shevchenko A, Mann M, Murray AW. 1998. Spindle checkpoint protein Xmad1 recruits Xmad2 to unattached kinetochores. *J. Cell Biol.* 143:283–95
53. Moyle MW, Kim T, Hattersley N, Espeut J, Cheerambathur DK, et al. 2014. A Bub1–Mad1 interaction targets the Mad1–Mad2 complex to unattached kinetochores to initiate the spindle checkpoint. *J. Cell Biol.* 204:647–57
54. London N, Biggins S. 2014. Mad1 kinetochore recruitment by Mps1-mediated phosphorylation of Bub1 signals the spindle checkpoint. *Genes Dev*. 28:140–52
55. Sironi L, Mapelli M, Knapp S, De Antoni A, Jeang KT, Musacchio A. 2002. Crystal structure of the tetrameric Mad1–Mad2 core complex: implications of a 'safety belt' binding mechanism for the spindle checkpoint. *EMBO J*. 21:2496–506
56. De Antoni A, Pearson CG, Cimini D, Canman JC, Sala V, et al. 2005. The Mad1/Mad2 complex as a template for Mad2 activation in the spindle assembly checkpoint. *Curr. Biol.* 15:214–25
57. Shah JV, Botvinick E, Bonday Z, Furnari F, Berns M, Cleveland DW. 2004. Dynamics of centromere and kinetochore proteins; implications for checkpoint signaling and silencing. *Curr. Biol.* 14:942–52
58. Yang M, Li B, Liu CJ, Tomchick DR, Machius M, et al. 2008. Insights into Mad2 regulation in the spindle checkpoint revealed by the crystal structure of the symmetric Mad2 dimer. *PLOS Biol*. 6:e50
59. Lara-Gonzalez P, Kim T, Oegema K, Corbett K, Desai A. 2021. A tripartite mechanism catalyzes Mad2-Cdc20 assembly at unattached kinetochores. *Science* 371:64–67
60. Piano V, Alex A, Stege P, Maffini S, Stoppiello GA, et al. 2021. CDC20 assists its catalytic incorporation in the mitotic checkpoint complex. *Science* 371:67–71
61. Kamenz J, Hauf S. 2017. Time to split up: dynamics of chromosome separation. *Trends Cell Biol*. 27:42–54
62. Ciosk R, Zachariae W, Michaelis C, Shevchenko A, Mann M, Nasmyth K. 1998. An ESP1/PDS1 complex regulates loss of sister chromatid cohesion at the metaphase to anaphase transition in yeast. *Cell* 93:1067–76
63. Orth M, Mayer B, Rehm K, Rothweiler U, Heidmann D, et al. 2011. Shugoshin is a Mad1/Cdc20-like interactor of Mad2. *EMBO J*. 30:2868–80
64. Hellmuth S, Gomez HL, Pendas AM, Stemmann O. 2020. Securin-independent regulation of separase by checkpoint-induced shugoshin-MAD2. *Nature* 580:536–41
65. Luo X, Tang Z, Xia G, Wassmann K, Matsumoto T, et al. 2004. The Mad2 spindle checkpoint protein has two distinct natively folded states. *Nat. Struct. Mol. Biol.* 11:338–45
66. Xia G, Luo X, Habu T, Rizo J, Matsumoto T, Yu H. 2004. Conformation-specific binding of p31^{comet} antagonizes the function of Mad2 in the spindle checkpoint. *EMBO J*. 23:3133–43
67. Défachelles L, Russo AE, Nelson CR, Bhalla N. 2020. The conserved AAA-ATPase PCH-2^{TRIP13} regulates spindle checkpoint strength. *Mol. Biol. Cell* 31:2219–33
68. Nelson CR, Hwang T, Chen PH, Bhalla N. 2015. TRIP13^{PCH-2} promotes Mad2 localization to unattached kinetochores in the spindle checkpoint response. *J. Cell Biol.* 211:503–16
69. Westhorpe FG, Tighe A, Lara-Gonzalez P, Taylor SS. 2011. p31^{comet}-mediated extraction of Mad2 from the MCC promotes efficient mitotic exit. *J. Cell Sci.* 124:3905–16
70. Teichner A, Eytan E, Sitry-Shevah D, Miniowitz-Shemtov S, Dumin E, et al. 2011. p31^{comet} promotes disassembly of the mitotic checkpoint complex in an ATP-dependent process. *PNAS* 108:3187–92
71. Jia L, Li B, Warrington RT, Hao X, Wang S, Yu H. 2011. Defining pathways of spindle checkpoint silencing: functional redundancy between Cdc20 ubiquitination and p31^{comet}. *Mol. Biol. Cell* 22:4227–35
72. Hagan RS, Manak MS, Buch HK, Meier MG, Meraldi P, et al. 2011. p31^{comet} acts to ensure timely spindle checkpoint silencing subsequent to kinetochore attachment. *Mol. Biol. Cell* 22:4236–46
73. Mo M, Arnaoutov A, Dasso M. 2015. Phosphorylation of *Xenopus* p31^{comet} potentiates mitotic checkpoint exit. *Cell Cycle* 14:3978–85
74. Hegemann B, Hutchins JR, Hudecz O, Novatchkova M, Rameseder J, et al. 2011. Systematic phosphorylation analysis of human mitotic protein complexes. *Sci. Signal.* 4:rs12
75. Date DA, Burrows AC, Summers MK. 2014. Phosphorylation regulates the p31^{Comet}-mitotic arrest-deficient 2 (Mad2) interaction to promote spindle assembly checkpoint (SAC) activity. *J. Biol. Chem.* 289:11367–73

76. Kaisari S, Shomer P, Ziv T, Sitry-Shevah D, Miniowitz-Shemtov S, et al. 2019. Role of Polo-like kinase 1 in the regulation of the action of p31^{comet} in the disassembly of mitotic checkpoint complexes. *PNAS* 116:11725–30
77. Lara-Gonzalez P, Moyle MW, Budrewicz J, Mendoza-Lopez J, Oegema K, Desai A. 2019. The G2-to-M transition is ensured by a dual mechanism that protects cyclin B from degradation by Cdc20-activated APC/C. *Dev. Cell* 51:313–25.e10
78. Lee SH, McCormick F, Saya H. 2010. Mad2 inhibits the mitotic kinesin MKlp2. *J. Cell Biol.* 191:1069–77
79. O'Neill TJ, Zhu Y, Gustafson TA. 1997. Interaction of MAD2 with the carboxyl terminus of the insulin receptor but not with the IGFIR. Evidence for release from the insulin receptor after activation. *J. Biol. Chem.* 272:10035–40
80. Choi E, Zhang X, Xing C, Yu H. 2016. Mitotic checkpoint regulators control insulin signaling and metabolic homeostasis. *Cell* 166:567–81
81. Marston AL, Amon A. 2004. Meiosis: cell-cycle controls shuffle and deal. *Nat. Rev. Mol. Cell Biol.* 5:983–97
82. Zickler D, Kleckner N. 1999. Meiotic chromosomes: integrating structure and function. *Annu. Rev. Genet.* 33:603–754
83. Hunter N. 2015. Meiotic recombination: the essence of heredity. *Cold Spring Harb. Perspect. Biol.* 7:a016618
84. Bhalla N, Dernburg AF. 2008. Prelude to a division. *Annu. Rev. Cell Dev. Biol.* 24:397–424
85. Keeney S, Lange J, Mohibullah N. 2014. Self-organization of meiotic recombination initiation: general principles and molecular pathways. *Annu. Rev. Genet.* 48:187–214
86. West AMV, Komives EA, Corbett KD. 2018. Conformational dynamics of the Hop1 HORMA domain reveal a common mechanism with the spindle checkpoint protein Mad2. *Nucleic Acids Res.* 46:279–92
87. West AM, Rosenberg SC, Ur SN, Lehmer MK, Ye Q, et al. 2019. A conserved filamentous assembly underlies the structure of the meiotic chromosome axis. *eLife* 8:e40372
88. Ferdous M, Higgins JD, Osman K, Lambing C, Roitinger E, et al. 2012. Inter-homolog crossing-over and synapsis in *Arabidopsis* meiosis are dependent on the chromosome axis protein AtASY3. *PLOS Genet.* 8:e1002507
89. Woltering D, Baumgartner B, Bagchi S, Larkin B, Loidl J, et al. 2000. Meiotic segregation, synapsis, and recombination checkpoint functions require physical interaction between the chromosomal proteins Red1p and Hop1p. *Mol. Cell. Biol.* 20:6646–58
90. Schalbetter SA, Fudenberg G, Baxter J, Pollard KS, Neale MJ. 2019. Principles of meiotic chromosome assembly revealed in *S. cerevisiae*. *Nat. Commun.* 10:4795
91. Alavattam KG, Maezawa S, Sakashita A, Khoury H, Barski A, et al. 2019. Attenuated chromatin compartmentalization in meiosis and its maturation in sperm development. *Nat. Struct. Mol. Biol.* 26:175–84
92. Patel L, Kang R, Rosenberg SC, Qiu Y, Raviram R, et al. 2019. Dynamic reorganization of the genome shapes the recombination landscape in meiotic prophase. *Nat. Struct. Mol. Biol.* 26:164–74
93. Wang Y, Wang H, Zhang Y, Du Z, Si W, et al. 2019. Reprogramming of meiotic chromatin architecture during spermatogenesis. *Mol. Cell* 73:547–61.e6
94. Sun X, Huang L, Markowitz TE, Blitzblau HG, Chen D, et al. 2015. Transcription dynamically patterns the meiotic chromosome-axis interface. *eLife* 4:e07424
95. Muller H, Scolari VF, Agier N, Piazza A, Thierry A, et al. 2018. Characterizing meiotic chromosomes' structure and pairing using a designer sequence optimized for Hi-C. *Mol. Syst. Biol.* 14:e8293
96. Fujiwara Y, Horisawa-Takada Y, Inoue E, Tani N, Shibuya H, et al. 2020. Meiotic cohesins mediate initial loading of HORMAD1 to the chromosomes and coordinate SC formation during meiotic prophase. *PLOS Genet.* 16:e1009048
97. Kim Y, Rosenberg SC, Kugel CL, Kostow N, Rog O, et al. 2014. The chromosome axis controls meiotic events through a hierarchical assembly of HORMA domain proteins. *Dev. Cell* 31:487–502
98. Severson AF, Ling L, van Zuylen V, Meyer BJ. 2009. The axial element protein HTP-3 promotes cohesin loading and meiotic axis assembly in *C. elegans* to implement the meiotic program of chromosome segregation. *Genes Dev.* 23:1763–78

99. Kohler S, Wojcik M, Xu K, Dernburg AF. 2017. Superresolution microscopy reveals the three-dimensional organization of meiotic chromosome axes in intact *Caenorhabditis elegans* tissue. *PNAS* 114:E4734–43
100. Daniel K, Lange J, Hached K, Fu J, Anastassiadis K, et al. 2011. Meiotic homologue alignment and its quality surveillance are controlled by mouse HORMAD1. *Nat. Cell. Biol.* 13:599–610
101. Shin YH, Choi Y, Erdin SU, Yatsenko SA, Kloc M, et al. 2010. Hormad1 mutation disrupts synaptonemal complex formation, recombination, and chromosome segregation in mammalian meiosis. *PLOS Genet.* 6:e1001190
102. Hollingsworth NM, Byers B. 1989. HOP1: a yeast meiotic pairing gene. *Genetics* 121:445–62
103. Panizza S, Mendoza MA, Berlinger M, Huang L, Nicolas A, et al. 2011. Spo11-accessory proteins link double-strand break sites to the chromosome axis in early meiotic recombination. *Cell* 146:372–83
104. Goodyer W, Kaitna S, Couteau F, Ward JD, Boulton SJ, Zetka M. 2008. HTP-3 links DSB formation with homolog pairing and crossing over during *C. elegans* meiosis. *Dev. Cell* 14:263–74
105. Rousova D, Nivsarkar V, Altmannova V, Funk SK, Raina VB, et al. 2020. Novel mechanistic insights into the role of Mer2 as the keystone of meiotic DNA break formation. bioRxiv 2020.07.30.228908 **https://doi.org/10.1101/2020.07.30.228908**
106. Stanzione M, Baumann M, Papanikos F, Dereli I, Lange J, et al. 2016. Meiotic DNA break formation requires the unsynapsed chromosome axis-binding protein IHO1 (CCDC36) in mice. *Nat. Cell. Biol.* 18:1208–20
107. Kariyazono R, Oda A, Yamada T, Ohta K. 2019. Conserved HORMA domain–containing protein Hop1 stabilizes interaction between proteins of meiotic DNA break hotspots and chromosome axis. *Nucleic Acids Res.* 47:10166–80
108. Claeys Bouuaert C, Pu S, Wang J, Oger C, Daccache D, et al. 2021. DNA-driven condensation assembles the meiotic DNA break machinery. *Nature* 592:144–49
109. Li J, Hooker GW, Roeder GS. 2006. *Saccharomyces cerevisiae* Mer2, Mei4 and Rec114 form a complex required for meiotic double-strand break formation. *Genetics* 173:1969–81
110. Sasanuma H, Murakami H, Fukuda T, Shibata T, Nicolas A, Ohta K. 2007. Meiotic association between Spo11 regulated by Rec102, Rec104 and Rec114. *Nucleic Acids Res.* 35:1119–33
111. Subramanian VV, Hochwagen A. 2014. The meiotic checkpoint network: step-by-step through meiotic prophase. *Cold Spring Harb. Perspect. Biol.* 6:a016675
112. Niu H, Wan L, Baumgartner B, Schaefer D, Loidl J, Hollingsworth NM. 2005. Partner choice during meiosis is regulated by Hop1-promoted dimerization of Mek1. *Mol. Biol. Cell* 16:5804–18
113. Latypov V, Rothenberg M, Lorenz A, Octobre G, Csutak O, et al. 2010. Roles of Hop1 and Mek1 in meiotic chromosome pairing and recombination partner choice in *Schizosaccharomyces pombe*. *Mol. Cell. Biol.* 30:1570–81
114. Sanchez-Moran E, Santos JL, Jones GH, Franklin FC. 2007. ASY1 mediates AtDMC1-dependent interhomolog recombination during meiosis in *Arabidopsis*. *Genes Dev.* 21:2220–33
115. Chuang CN, Cheng YH, Wang TF. 2012. Mek1 stabilizes Hop1-Thr318 phosphorylation to promote interhomolog recombination and checkpoint responses during yeast meiosis. *Nucleic Acids Res.* 40:11416–27
116. Subramanian VV, MacQueen AJ, Vader G, Shinohara M, Sanchez A, et al. 2016. Chromosome synapsis alleviates Mek1-dependent suppression of meiotic DNA repair. *PLOS Biol.* 14:e1002369
117. Carballo JA, Johnson AL, Sedgwick SG, Cha RS. 2008. Phosphorylation of the axial element protein Hop1 by Mec1/Tel1 ensures meiotic interhomolog recombination. *Cell* 132:758–70
118. Niu H, Li X, Job E, Park C, Moazed D, et al. 2007. Mek1 kinase is regulated to suppress double-strand break repair between sister chromatids during budding yeast meiosis. *Mol. Cell. Biol.* 27:5456–67
119. Niu H, Wan L, Busygina V, Kwon Y, Allen JA, et al. 2009. Regulation of meiotic recombination via Mek1-mediated Rad54 phosphorylation. *Mol. Cell* 36:393–404
120. Govin J, Dorsey J, Gaucher J, Rousseaux S, Khochbin S, Berger SL. 2010. Systematic screen reveals new functional dynamics of histones H3 and H4 during gametogenesis. *Genes Dev.* 24:1772–86
121. Yang C, Hu B, Portheine SM, Chuenban P, Schnittger A. 2020. State changes of the HORMA protein ASY1 are mediated by an interplay between its closure motif and PCH2. *Nucleic Acids Res.* 48:11521–35

122. Raina VB, Vader G. 2020. Homeostatic control of meiotic prophase checkpoint function by Pch2 and Hop1. *Curr. Biol.* 30:4413–24.e5
123. Miao C, Tang D, Zhang H, Wang M, Li Y, et al. 2013. CENTRAL REGION COMPONENT1, a novel synaptonemal complex component, is essential for meiotic recombination initiation in rice. *Plant Cell* 25:2998–3009
124. Herruzo E, Lago-Maciel A, Baztán S, Santos B, Carballo JA, et al. 2021. Pch2 orchestrates the meiotic recombination checkpoint from the cytoplasm. *PLOS Genet.* 17:e1009560
125. Li XC, Schimenti JC. 2007. Mouse pachytene checkpoint 2 (trip13) is required for completing meiotic recombination but not synapsis. *PLOS Genet*. 3:e130
126. Loidl J. 2016. Conservation and variability of meiosis across the eukaryotes. *Annu. Rev. Genet.* 50:293–316
127. Cahoon CK, Hawley RS. 2016. Regulating the construction and demolition of the synaptonemal complex. *Nat. Struct. Mol. Biol.* 23:369–77
128. Vader G. 2015. Pch2^{TRIP13}: controlling cell division through regulation of HORMA domains. *Chromosoma* 124:333–39
129. Lambing C, Osman K, Nuntasoontorn K, West A, Higgins JD, et al. 2015. Arabidopsis PCH2 mediates meiotic chromosome remodeling and maturation of crossovers. *PLOS Genet*. 11:e1005372
130. Giacopazzi S, Vong D, Devigne A, Bhalla N. 2020. PCH-2 collaborates with CMT-1 to proofread meiotic homolog interactions. *PLOS Genet*. 16:e1008904
131. Ji J, Tang D, Shen Y, Xue Z, Wang H, et al. 2016. P31^{comet}, a member of the synaptonemal complex, participates in meiotic DSB formation in rice. *PNAS* 113:10577–82
132. Balboni M, Yang C, Komaki S, Brun J, Schnittger A. 2020. COMET functions as a PCH2 cofactor in regulating the HORMA domain protein ASY1. *Curr. Biol.* 30:4113–27.e6
133. van Hooff JJ, Tromer E, van Wijk LM, Snel B, Kops GJ. 2017. Evolutionary dynamics of the kinetochore network in eukaryotes as revealed by comparative genomics. *EMBO Rep*. 18:1559–71
134. Chen C, Jomaa A, Ortega J, Alani EE. 2014. Pch2 is a hexameric ring ATPase that remodels the chromosome axis protein Hop1. *PNAS* 111:E44–53
135. Villar-Fernandez MA, Cardoso da Silva R, Firlej M, Pan D, Weir E, et al. 2020. Biochemical and functional characterization of a meiosis-specific Pch2/ORC AAA+ assembly. *Life Sci. Alliance* 3:e201900630
136. Nelson JR, Lawrence CW, Hinkle DC. 1996. Deoxycytidyl transferase activity of yeast REV1 protein. *Nature* 382:729–31
137. Nelson JR, Lawrence CW, Hinkle DC. 1996. Thymine-thymine dimer bypass by yeast DNA polymerase ζ. *Science* 272:1646–49
138. Johnson RE, Prakash L, Prakash S. 2012. Pol31 and Pol32 subunits of yeast DNA polymerase δ are also essential subunits of DNA polymerase ζ. *PNAS* 109:12455–60
139. Murakumo Y, Roth T, Ishii H, Rasio D, Numata S, et al. 2000. A human REV7 homolog that interacts with the polymerase ζ catalytic subunit hREV3 and the spindle assembly checkpoint protein hMAD2. *J. Biol. Chem.* 275:4391–97
140. Sale JE. 2013. Translesion DNA synthesis and mutagenesis in eukaryotes. *Cold Spring Harb. Perspect. Biol.* 5:a012708
141. Hara K, Shimizu T, Unzai S, Akashi S, Sato M, Hashimoto H. 2009. Purification, crystallization and initial X-ray diffraction study of human REV7 in complex with a REV3 fragment. *Acta Crystallogr. Sect. F Struct. Biol. Cryst. Commun.* 65:1302–5
142. Hara K, Hashimoto H, Murakumo Y, Kobayashi S, Kogame T, et al. 2010. Crystal structure of human REV7 in complex with a human REV3 fragment and structural implication of the interaction between DNA polymerase ζ and REV1. *J. Biol. Chem.* 285:12299–307
143. Tomida J, Takata K, Lange SS, Schibler AC, Yousefzadeh MJ, et al. 2015. REV7 is essential for DNA damage tolerance via two REV3L binding sites in mammalian DNA polymerase ζ. *Nucleic Acids Res.* 43:1000–11
144. Rizzo AA, Vassel FM, Chatterjee N, D'Souza S, Li Y, et al. 2018. Rev7 dimerization is important for assembly and function of the Rev1/Polζ translesion synthesis complex. *PNAS* 115:E8191–200
145. Malik R, Kopylov M, Gomez-Llorente Y, Jain R, Johnson RE, et al. 2020. Structure and mechanism of B-family DNA polymerase ζ specialized for translesion DNA synthesis. *Nat. Struct. Mol. Biol.* 27:913–24

146. Du Truong C, Craig TA, Cui G, Victoria Botuyan M, Serkasevich RA, et al. 2021. Cryo-EM reveals conformational flexibility in apo DNA polymerase ζ . *J. Biol. Chem.* 297:100912
147. Wojtaszek J, Lee CJ, D'Souza S, Minesinger B, Kim H, et al. 2012. Structural basis of Rev1-mediated assembly of a quaternary vertebrate translesion polymerase complex consisting of Rev1, heterodimeric polymerase (Pol) ζ , and Pol κ. *J. Biol. Chem.* 287:33836–46
148. Pustovalova Y, Bezsonova I, Korzhnev DM. 2012. The C-terminal domain of human Rev1 contains independent binding sites for DNA polymerase η and Rev7 subunit of polymerase ζ . *FEBS Lett.* 586:3051–56
149. Pozhidaeva A, Pustovalova Y, D'Souza S, Bezsonova I, Walker GC, Korzhnev DM. 2012. NMR structure and dynamics of the C-terminal domain from human Rev1 and its complex with Rev1 interacting region of DNA polymerase η. *Biochemistry* 51:5506–20
150. Ohashi E, Hanafusa T, Kamei K, Song I, Tomida J, et al. 2009. Identification of a novel REV1-interacting motif necessary for DNA polymerase κ function. *Genes Cells* 14:101–11
151. Jain R, Aggarwal AK, Rechkoblit O. 2018. Eukaryotic DNA polymerases. *Curr. Opin. Struct. Biol.* 53:77–87
152. Prakash S, Johnson RE, Prakash L. 2005. Eukaryotic translesion synthesis DNA polymerases: specificity of structure and function. *Annu. Rev. Biochem.* 74:317–53
153. Xu G, Chapman JR, Brandsma I, Yuan J, Mistrik M, et al. 2015. REV7 counteracts DNA double-strand break resection and affects PARP inhibition. *Nature* 521:541–44
154. Noordermeer SM, Adam S, Setiaputra D, Barazas M, Pettitt SJ, et al. 2018. The shieldin complex mediates 53BP1-dependent DNA repair. *Nature* 560:117–21
155. Mirman Z, Lottersberger F, Takai H, Kibe T, Gong Y, et al. 2018. 53BP1-RIF1-shieldin counteracts DSB resection through CST- and Polα-dependent fill-in. *Nature* 560:112–16
156. Ghezraoui H, Oliveira C, Becker JR, Bilham K, Moralli D, et al. 2018. 53BP1 cooperation with the REV7-shieldin complex underpins DNA structure-specific NHEJ. *Nature* 560:122–27
157. Barazas M, Annunziato S, Pettitt SJ, de Krijger I, Ghezraoui H, et al. 2018. The CST complex mediates end protection at double-strand breaks and promotes PARP inhibitor sensitivity in BRCA1-deficient cells. *Cell Rep.* 23:2107–18
158. Setiaputra D, Durocher D. 2019. Shieldin – the protector of DNA ends. *EMBO Rep.* 20:e47560
159. Sarangi P, Clairmont CS, Galli LD, Moreau LA, D'Andrea AD. 2020. p31^{comet} promotes homologous recombination by inactivating REV7 through the TRIP13 ATPase. *PNAS* 117:26795–803
160. Chen J, Fang G. 2001. MAD2B is an inhibitor of the anaphase-promoting complex. *Genes Dev.* 15:1765–70
161. Pfleger CM, Salic A, Lee E, Kirschner MW. 2001. Inhibition of Cdh1-APC by the MAD2-related protein MAD2L2: a novel mechanism for regulating Cdh1. *Genes Dev.* 15:1759–64
162. Listovsky T, Sale JE. 2013. Sequestration of CDH1 by MAD2L2 prevents premature APC/C activation prior to anaphase onset. *J. Cell Biol.* 203:87–100
163. Medendorp K, van Groningen JJ, Vreede L, Hetterschijt L, van den Hurk WH, et al. 2009. The mitotic arrest deficient protein MAD2B interacts with the small GTPase RAN throughout the cell cycle. *PLOS ONE* 4:e7020
164. Wang X, Pernicone N, Pertz L, Hua D, Zhang T, et al. 2019. REV7 has a dynamic adaptor region to accommodate small GTPase RAN/*Shigella* IpaB ligands, and its activity is regulated by the RanGTP/GDP switch. *J. Biol. Chem.* 294:15733–42
165. Hara K, Taharazako S, Ikeda M, Fujita H, Mikami Y, et al. 2017. Dynamic feature of mitotic arrest deficient 2-like protein 2 (MAD2L2) and structural basis for its interaction with chromosome alignment-maintaining phosphoprotein (CAMP). *J. Biol. Chem.* 292:17658–67
166. Iwai H, Kim M, Yoshikawa Y, Ashida H, Ogawa M, et al. 2007. A bacterial effector targets Mad2L2, an APC inhibitor, to modulate host cell cycling. *Cell* 130:611–23
167. Mizushima N. 2010. The role of the Atg1/ULK1 complex in autophagy regulation. *Curr. Opin. Cell Biol.* 22:132–39
168. Stephan JS, Yeh YY, Ramachandran V, Deminoff SJ, Herman PK. 2009. The Tor and PKA signaling pathways independently target the Atg1/Atg13 protein kinase complex to control autophagy. *PNAS* 106:17049–54

169. Kamada Y, Yoshino K, Kondo C, Kawamata T, Oshiro N, et al. 2010. Tor directly controls the Atg1 kinase complex to regulate autophagy. *Mol. Cell. Biol.* 30:1049–58
170. Puente C, Hendrickson RC, Jiang X. 2016. Nutrient-regulated phosphorylation of ATG13 inhibits starvation-induced autophagy. *J. Biol. Chem.* 291:6026–35
171. Fujioka Y, Suzuki SW, Yamamoto H, Kondo-Kakuta C, Kimura Y, et al. 2014. Structural basis of starvation-induced assembly of the autophagy initiation complex. *Nat. Struct. Mol. Biol.* 21:513–21
172. Yamamoto H, Fujioka Y, Suzuki SW, Noshiro D, Suzuki H, et al. 2016. The intrinsically disordered protein Atg13 mediates supramolecular assembly of autophagy initiation complexes. *Dev. Cell* 38:86–99
173. Shi X, Yokom AL, Wang C, Young LN, Youle RJ, Hurley JH. 2020. ULK complex organization in autophagy by a C-shaped FIP200 N-terminal domain dimer. *J. Cell Biol.* 219:e201911047
174. Scott SV, Nice DC 3rd, Nau JJ, Weisman LS, Kamada Y, et al. 2000. Apg13p and Vac8p are part of a complex of phosphoproteins that are required for cytoplasm to vacuole targeting. *J. Biol. Chem.* 275:25840–49
175. Hollenstein DM, Gomez-Sanchez R, Ciftci A, Kriegenburg F, Mari M, et al. 2019. Vac8 spatially confines autophagosome formation at the vacuole in *S. cerevisiae*. *J. Cell Sci.* 132:jcs235002
176. Fujioka Y, Alam JM, Noshiro D, Mouri K, Ando T, et al. 2020. Phase separation organizes the site of autophagosome formation. *Nature* 578:301–5
177. Memisoglu G, Eapen VV, Yang Y, Klionsky DJ, Haber JE. 2019. PP2C phosphatases promote autophagy by dephosphorylation of the Atg1 complex. *PNAS* 116:1613–20
178. Park JM, Jung CH, Seo M, Otto NM, Grunwald D, et al. 2016. The ULK1 complex mediates MTORC1 signaling to the autophagy initiation machinery via binding and phosphorylating ATG14. *Autophagy* 12:547–64
179. Yamamoto H, Kakuta S, Watanabe TM, Kitamura A, Sekito T, et al. 2012. Atg9 vesicles are an important membrane source during early steps of autophagosome formation. *J. Cell Biol.* 198:219–33
180. Wallot-Hieke N, Verma N, Schlutermann D, Berleth N, Deitersen J, et al. 2018. Systematic analysis of ATG13 domain requirements for autophagy induction. *Autophagy* 14:743–63
181. Suzuki SW, Yamamoto H, Oikawa Y, Kondo-Kakuta C, Kimura Y, et al. 2015. Atg13 HORMA domain recruits Atg9 vesicles during autophagosome formation. *PNAS* 112:3350–55
182. Rao Y, Perna MG, Hofmann B, Beier V, Wollert T. 2016. The Atg1–kinase complex tethers Atg9-vesicles to initiate autophagy. *Nat. Commun.* 7:10338
183. Gordon DJ, Resio B, Pellman D. 2012. Causes and consequences of aneuploidy in cancer. *Nat. Rev. Genet.* 13:189–203
184. Sotillo R, Hernando E, Diaz-Rodriguez E, Teruya-Feldstein J, Cordon-Cardo C, et al. 2007. Mad2 overexpression promotes aneuploidy and tumorigenesis in mice. *Cancer Cell* 11:9–23
185. Chen YT, Venditti CA, Theiler G, Stevenson BJ, Iseli C, et al. 2005. Identification of CT46/HORMAD1, an immunogenic cancer/testis antigen encoding a putative meiosis-related protein. *Cancer Immun.* 5:9
186. Aung PP, Oue N, Mitani Y, Nakayama H, Yoshida K, et al. 2006. Systematic search for gastric cancer-specific genes based on SAGE data: Melanoma inhibitory activity and matrix metalloproteinase-10 are novel prognostic factors in patients with gastric cancer. *Oncogene* 25:2546–57
187. Nichols BA, Oswald NW, McMillan EA, McGlynn K, Yan J, et al. 2018. HORMAD1 is a negative prognostic indicator in lung adenocarcinoma and specifies resistance to oxidative and genotoxic stress. *Cancer Res.* 78:6196–208
188. Gao Y, Kardos J, Yang Y, Tamir TY, Mutter-Rottmayer E, et al. 2018. The cancer/testes (CT) antigen HORMAD1 promotes homologous recombinational DNA repair and radioresistance in lung adenocarcinoma cells. *Sci. Rep.* 8:15304
189. Adelaide J, Finetti P, Bekhouche I, Repellini L, Geneix J, et al. 2007. Integrated profiling of basal and luminal breast cancers. *Cancer Res.* 67:11565–75
190. Yao J, Caballero OL, Yung WK, Weinstein JN, Riggins GJ, et al. 2014. Tumor subtype-specific cancer—testis antigens as potential biomarkers and immunotherapeutic targets for cancers. *Cancer Immunol. Res.* 2:371–79
191. Watkins J, Weekes D, Shah V, Gazinska P, Joshi S, et al. 2015. Genomic complexity profiling reveals that HORMAD1 overexpression contributes to homologous recombination deficiency in triple-negative breast cancers. *Cancer Discov.* 5:488–505

192. Holm K, Staaf J, Lauss M, Aine M, Lindgren D, et al. 2016. An integrated genomics analysis of epigenetic subtypes in human breast tumors links DNA methylation patterns to chromatin states in normal mammary cells. *Breast Cancer Res.* 18:27
193. Wang X, Tan Y, Cao X, Kim JA, Chen T, et al. 2018. Epigenetic activation of HORMAD1 in basal-like breast cancer: role in Rucaparib sensitivity. *Oncotarget* 9:30115–27
194. Lin Q, Hou S, Guan F, Lin C. 2018. HORMAD2 methylation-mediated epigenetic regulation of gene expression in thyroid cancer. *J. Cell Mol. Med.* 22:4640–52
195. Liu M, Chen J, Hu L, Shi X, Zhou Z, et al. 2012. HORMAD2/CT46.2, a novel cancer/testis gene, is ectopically expressed in lung cancer tissues. *Mol. Hum. Reprod.* 18:599–604
196. Liu K, Wang Y, Zhu Q, Li P, Chen J, et al. 2020. Aberrantly expressed HORMAD1 disrupts nuclear localization of MCM8–MCM9 complex and compromises DNA mismatch repair in cancer cells. *Cell Death Dis.* 11:519
197. Boersma V, Moatti N, Segura-Bayona S, Peuscher MH, van der Torre J, et al. 2015. MAD2L2 controls DNA repair at telomeres and DNA breaks by inhibiting 5′ end resection. *Nature* 521:537–40
198. Tomida J, Takata KI, Bhetawal S, Person MD, Chao HP, et al. 2018. FAM35A associates with REV7 and modulates DNA damage responses of normal and BRCA1-defective cells. *EMBO J.* 37:e99543
199. Vassel FM, Bian K, Walker GC, Hemann MT. 2020. Rev7 loss alters cisplatin response and increases drug efficacy in chemotherapy-resistant lung cancer. *PNAS* 117:28922–24
200. Niimi K, Murakumo Y, Watanabe N, Kato T, Mii S, et al. 2014. Suppression of REV7 enhances cisplatin sensitivity in ovarian clear cell carcinoma cells. *Cancer Sci.* 105:545–52
201. Chatterjee N, Whitman MA, Harris CA, Min SM, Jonas O, et al. 2020. REV1 inhibitor JH-RE-06 enhances tumor cell response to chemotherapy by triggering senescence hallmarks. *PNAS* 117:28918–21
202. Rhodes DR, Yu J, Shanker K, Deshpande N, Varambally R, et al. 2004. Large-scale meta-analysis of cancer microarray data identifies common transcriptional profiles of neoplastic transformation and progression. *PNAS* 101:9309–14
203. Carter SL, Eklund AC, Kohane IS, Harris LN, Szallasi Z. 2006. A signature of chromosomal instability inferred from gene expression profiles predicts clinical outcome in multiple human cancers. *Nat. Genet.* 38:1043–48
204. Dazhi W, Mengxi Z, Fufeng C, Meixing Y. 2017. Elevated expression of thyroid hormone receptor-interacting protein 13 drives tumorigenesis and affects clinical outcome. *Biomark. Med.* 11:19–31
205. Ju L, Li X, Shao J, Lu R, Wang Y, Bian Z. 2018. Upregulation of thyroid hormone receptor interactor 13 is associated with human hepatocellular carcinoma. *Oncol. Rep.* 40:3794–802
206. Yao J, Zhang X, Li J, Zhao D, Gao B, et al. 2018. Silencing TRIP13 inhibits cell growth and metastasis of hepatocellular carcinoma by activating of TGF-β1/smad3. *Cancer Cell Int.* 18:208
207. Wang D, Liu J, Liu S, Li W. 2020. Identification of crucial genes associated with immune cell infiltration in hepatocellular carcinoma by weighted gene co-expression network analysis. *Front. Genet.* 11:342
208. Martin KJ, Patrick DR, Bissell MJ, Fournier MV. 2008. Prognostic breast cancer signature identified from 3D culture model accurately predicts clinical outcome across independent datasets. *PLOS ONE* 3:e2994
209. Maurizio E, Wisniewski JR, Ciani Y, Amato A, Arnoldo L, et al. 2016. Translating proteomic into functional data: An high mobility group A1 (HMGA1) proteomic signature has prognostic value in breast cancer. *Mol. Cell Proteom.* 15:109–23
210. Nieto-Jimenez C, Alcaraz-Sanabria A, Paez R, Perez-Pena J, Corrales-Sanchez V, et al. 2017. DNA-damage related genes and clinical outcome in hormone receptor positive breast cancer. *Oncotarget* 8:62834–41
211. Zhang Y, Xue Q, Pan G, Meng QH, Tuo X, et al. 2017. Integrated analysis of genome-wide copy number alterations and gene expression profiling of lung cancer in Xuanwei, China. *PLOS ONE* 12:e0169098
212. Li W, Zhang G, Li X, Wang X, Li Q, et al. 2018. Thyroid hormone receptor interactor 13 (TRIP13) overexpression associated with tumor progression and poor prognosis in lung adenocarcinoma. *Biochem. Biophys. Res. Commun.* 499:416–24
213. Zhang Q, Dong Y, Hao S, Tong Y, Luo Q, Aerxiding P. 2019. The oncogenic role of TRIP13 in regulating proliferation, invasion, and cell cycle checkpoint in NSCLC cells. *Int. J. Clin. Exp. Pathol.* 12:3357–66

214. Abdul Aziz NA, Mokhtar NM, Harun R, Mollah MM, Mohamed Rose I, et al. 2016. A 19-gene expression signature as a predictor of survival in colorectal cancer. *BMC Med. Genom.* 9:58
215. Kurita K, Maeda M, Mansour MA, Kokuryo T, Uehara K, et al. 2016. TRIP13 is expressed in colorectal cancer and promotes cancer cell invasion. *Oncol. Lett.* 12:5240–46
216. Sheng N, Yan L, Wu K, You W, Gong J, et al. 2018. TRIP13 promotes tumor growth and is associated with poor prognosis in colorectal cancer. *Cell Death Dis.* 9:402
217. Larkin SE, Holmes S, Cree IA, Walker T, Basketter V, et al. 2012. Identification of markers of prostate cancer progression using candidate gene expression. *Br. J. Cancer* 106:157–65
218. van Kester MS, Borg MK, Zoutman WH, Out-Luiting JJ, Jansen PM, et al. 2012. A meta-analysis of gene expression data identifies a molecular signature characteristic for tumor-stage mycosis fungoides. *J. Invest. Dermatol.* 132:2050–59
219. Tao Y, Yang G, Yang H, Song D, Hu L, et al. 2017. TRIP13 impairs mitotic checkpoint surveillance and is associated with poor prognosis in multiple myeloma. *Oncotarget* 8:26718–31
220. Zhou K, Zhang W, Zhang Q, Gui R, Zhao H, et al. 2017. Loss of thyroid hormone receptor interactor 13 inhibits cell proliferation and survival in human chronic lymphocytic leukemia. *Oncotarget* 8:25469–81
221. Dong L, Ding H, Li Y, Xue D, Li Z, et al. 2019. TRIP13 is a predictor for poor prognosis and regulates cell proliferation, migration and invasion in prostate cancer. *Int. J. Biol. Macromol.* 121:200–6
222. Liu M, Qiu YL, Jin T, Zhou Y, Mao ZY, Zhang YJ. 2018. Meta-analysis of microarray datasets identify several chromosome segregation-related cancer/testis genes potentially contributing to anaplastic thyroid carcinoma. *PeerJ* 6:e5822
223. Yan X, Guo ZX, Liu XP, Feng YJ, Zhao YJ, et al. 2019. Four novel biomarkers for bladder cancer identified by weighted gene coexpression network analysis. *J. Cell Physiol.* 234:19073–87
224. Di S, Li M, Ma Z, Guo K, Li X, Yan X. 2019. TRIP13 upregulation is correlated with poor prognosis and tumor progression in esophageal squamous cell carcinoma. *Pathol. Res. Pract.* 215:152415
225. Gao Y, Liu S, Guo Q, Zhang S, Zhao Y, et al. 2019. Increased expression of TRIP13 drives the tumorigenesis of bladder cancer in association with the EGFR signaling pathway. *Int. J. Biol. Sci.* 15:1488–99
226. Lu S, Guo M, Fan Z, Chen Y, Shi X, et al. 2019. Elevated TRIP13 drives cell proliferation and drug resistance in bladder cancer. *Am. J. Transl. Res.* 11:4397–410
227. Niu L, Gao Z, Cui Y, Yang X, Li H. 2019. Thyroid receptor-interacting protein 13 is correlated with progression and poor prognosis in bladder cancer. *Med. Sci. Monit.* 25:6660–68
228. Yu L, Xiao Y, Zhou X, Wang J, Chen S, et al. 2019. TRIP13 interference inhibits the proliferation and metastasis of thyroid cancer cells through regulating TTC5/p53 pathway and epithelial-mesenchymal transition related genes expression. *Biomed. Pharmacother.* 120:109508
229. Wang Y, Huang J, Li B, Xue H, Tricot G, et al. 2020. A small-molecule inhibitor targeting TRIP13 suppresses multiple myeloma progression. *Cancer Res.* 80:536–48
230. Banerjee R, Russo N, Liu M, Basrur V, Bellile E, et al. 2014. TRIP13 promotes error-prone nonhomologous end joining and induces chemoresistance in head and neck cancer. *Nat. Commun.* 5:4527
231. Yost S, de Wolf B, Hanks S, Zachariou A, Marcozzi C, et al. 2017. Biallelic TRIP13 mutations predispose to Wilms tumor and chromosome missegregation. *Nat. Genet.* 49:1148–51
232. Xie W, Yang X, Xu M, Jiang T. 2012. Structural insights into the assembly of human translesion polymerase complexes. *Protein Cell* 3:864–74
233. Dev H, Chiang TW, Lescale C, de Krijger I, Martin AG, et al. 2018. Shieldin complex promotes DNA end-joining and counters homologous recombination in BRCA1-null cells. *Nat. Cell. Biol.* 20:954–65
234. Marks DH, Thomas R, Chin Y, Shah R, Khoo C, Benezra R. 2017. Mad2 overexpression uncovers a critical role for TRIP13 in mitotic exit. *Cell Rep.* 19:1832–45